Ulm University

Institute of Clinical and Experimental Trauma Immunology

Director: Prof. Dr. med. Markus Huber-Lang

The Inflammatory Response of the Liver after Polytrauma Promotes the Increase in the Secretion of Bone-related Modifiers

Dissertation

for the attainment of the doctorate of medicine (Dr. med.)

of the Medical Faculty of the Ulm University

submitted by

Yang Li

born in Siyang

2022

Dean of the Faculty of Medicine: Prof. Dr. rer. nat. Thomas Wirth

1. Reviewer: Prof. Dr. Markus Huber-Lang

2. Reviewer: Prof. Dr. Melanie Haffner-Luntzer

Day of promotion: February 17, 2023

For my mother

CONTENTS

List of Abbreviations

ALP	alkaline phosphatase
ALT	aspartate transaminase
ARDS	acute respiratory distress syndrome
AST	alanine aminotransferase
ATP	adenosine triphosphate
BCA	bicinchoninic acid
BSA	bovine serum albumin
BW	body weight
C5	complement component 5
CD	cluster of differentiation
cDNA	complementary deoxyribonucleic acid
CVP	central venous pressure
DAMPs	damage-associated molecular patterns
DEPC	diethyl pyrocarbonate
DNA	deoxyribonucleic acid
EC	Endothelial cell
ECG	electrocardiography
EDTA	Ethylenediaminetetraacetic acid
ELISA	Enzyme-Linked Immuno Sorbent Assay
Fig	Figure
GAPDH	glyceraldehyde-3-phosphate dehydrogenase
GGT	γ-glutamyl transferase

HE	haematoxylin and eosin
HIF	hypoxia-inducible transcription factor
HMGB-1	High-Mobility-Group-Protein Box 1
HS	haemorrhagic shock
HSC	Hepatic Stellate Cell
i.m.	intramuscular injection
ICAM-1	intercellular cell adhesion molecule-1
ICU	Intensive care unit
IL	interleukin
IRI	ischaemia-reperfusion injury
KCs	Kupffer Cells
L-FABP	liver type fatty acid-binding protein
MAPK	mitogen-activated protein kinase
MIP-2	macrophage inflammatory protein-2
MOF	Multiple Organ failure
MPO	Myeloperoxidase
mRNA	messenger ribonucleic acid
NADPH	nicotinamide adenine dinucleotide phosphate
NF-κB	nuclear factor-κB
NK cells	natural killer cells
NO	nitric oxide
OCN	osteocalcin
OPG	osteoprotegerin
OPN	osteopontin

PAMPs	pathogen-associated molecular patterns
PBS	phosphate buffered saline
P_{insp}	inspiratory pressure
PMN	neutrophil (polymorphonuclear leukocyte)
PRRs	pattern recognition receptors
PT	polytrauma
PT + HS	polytrauma + haemorrhagic shock
PTH	parathyroid hormone
RANK	receptor activator of nuclear factor-κB
RANKL	receptor activator of nuclear factor-κB-ligand
RNA	ribonucleic acid
ROS	reactive oxygen species
ROX	carboxy-X-rhodamine
RT-qPCR	real time quantitative polymerase chain reaction
SAP	Serum Amyloid protein P
SD	standard deviation
TBI	traumatic brain injury
TBS	tris-buffered saline
TBST	tris-buffered saline with 10% Tween
TGF-β	transforming growth factor beta
TLRs	toll-like receptors
TMB	Tetramethylbenzidine
TNF	tumour necrosis factor
Txt	blunt chest trauma

VCAM	vascular cell adhesion molecule

List of Symbols

%	percent
℃	degree Celsius
g	gram
h	hour
kg	kilogram
M	molar
mg	milligram
min	minute
ml	milliliter
mM	millimolar
mmHg	millimeter of mercury
nM	nanomolar
μg	microgram
μl	microliter
μM	micromolar

1 Introduction

Polytrauma is defined as an injury to two or more parts of the body as a result of violent factors, at least one or the sum of all injuries of which are potentially life-threatening [29, 102]. As treatment concepts continue to evolve and clinical practice continues to progress, trauma and its complications continue to be one of the leading causes of death among young and middle-aged people [18]. The liver is protected by the ribcage arch to avoid or reduce the impact of external mechanical trauma force. Nevertheless, statistics show that liver injuries account for approximately 66% of all abdominal trauma [6, 20]. Hepatic injuries can be graded according to the location and severity of the injury. After liver injury has occurred, the surgeon needs to carefully consider how much strategy can be applied on patients and medicals, depending on the patient's vital signs, complications and blood gas analysis [127]. The liver is an important endocrine organ, which not only involved in the body's metabolic activities, but is also involved in the removal of harmful factors that damage the body. Thus, trauma-induced impairment of liver function does not only affect the functional repair of the liver itself, but also other tissues and organs [42, 158, 168]. As the liver is the main organ of the body's metabolism, it is necessary to positively consider the various factors that can damage the liver after trauma and to identify effective measures to prevent any remaining visceral damage that may occur. Encouragingly, improvements in diagnostic methods and updated treatment guidelines have led to a reduction in mortality due to liver trauma. The overall mortality rate for these patients is currently around 10% [103].

The individual dysfunction of the liver and other organs caused by liver injury involves complex pathophysiological mechanisms, which are still not well understood. Current research focuses on the following areas: ischaemia-reperfusion injury, inflammatory response of the liver and apoptosis [61, 145]. Therefore, a systematic understanding of the pathological changes and inflammatory response of the liver

after trauma is necessary and beneficial for the prevention and resolution of various clinical problems resulting from liver injury.

1.1 Trauma

1.1.1 The Epidemiology of Trauma

Although mortality due to trauma has declined significantly in developed countries with the advancement of modern medical technology, improved diagnosis and a better medical environment, trauma remains a common contributor to death in young people under the age of 40 [13, 109, 171]. The World Health Organization evaluated about 5.8 million annual deaths worldwide by trauma [45, 74]. The high incidence of the disease pattern not only brings misfortune to individuals and families but also places a heavy burden on society. According to statistics, the total economic cost of traffic accidents in China in 2017 was 72.6 billion US $, equivalent to 0.60% of its gross national product in that year [140].

Research data shows that the highest incidence of trauma is within the 25-54 age group . The traffic accidents and fall-related injuries are the main causes of death. Additionally, the areas most likely to be injured after trauma are, in order, the brain, lower extremity, upper extremity, chest and abdomen [155]. Trauma-related mortality is usually described as trimodal: instantaneous (minutes), early (hours), and long-term (days to weeks). A retrospective study has shown that more than 50% of deaths within 48h of admission due to trauma are due to uncontrolled exsanguination after injury [33]. Development of multiple organ failure (MOF) was the most common cause of death in the late stages (61%) [124]. For the long-term (after 7 days) causes of death, the MOF was reported as the main cause of death in several studies until the end of the last century [5, 96, 115]. However, there is an increasing body of evidence that traumatic brain injury (TBI) is the leading cause of death in post-traumatic patients

[116]. In Germany, trauma-related mortality rates are polytrauma (45.7%), TBI (38%), exsanguination (9.5%) and blunt chest trauma (3.2%) [67].

Initial tissue damage, exsanguination and subsequent secondary remote organ injury induce local and systemic production of endogenous mediators that can operate as danger signals, mediators and damage clearance promoters. With release of damage-associated molecular patterns (DAMPs) [27]. Recognition of DAMPs by the innate immune system triggers both an intense pro-inflammatory immune response and a concomitant anti-inflammatory response [27, 87]. Numerous previous studies have confirmed that excessive inflammation causes damage not only to the tissues at the original trauma site but also to the distal non-traumatized organs [7, 10, 11, 107]. Further, the anti-inflammatory response leads to impaired host defences and sepsis, which together can lead to multiple organ dysfunctions and ultimately to death [167].

1.1.2 Blunt Chest Trauma

Blunt chest trauma (Txt) may lead to a miserable condition frequently linked to structural damage and impaired blood oxygenation. Txt is often not identified until after death [24, 134]. The pathological mechanisms of Txt include injury to tissue (endothelial and epithelial cells), inflammatory response, increased pulmonary microvascular permeability, pulmonary edema, dysfunction of surface active substances, dysfunction of the ventilation/blood flow ratio, reduced lung compliance and problems in oxygenation [89, 101].

The Txt is the third most common injury in polytrauma patients following head and extremities injuries [131, 138]. It is worth illustrating that blunt pulmonary contusions are often associated with multiple injuries, which means that they cause a high mortality and disability rate in patients [152]. Because pulmonary contusions are mostly caused by strong violence, patients often have rib fractures,

hematopneumothorax or other organ injuries, thus increasing the severity and complexity of the injury [135]. Most patients recover within 7 days after injury with aggressive comprehensive supportive therapy, resulting in a morbidity and mortality rate of 10-20% [83]. If not treated properly early, it could arise further to develop acute respiratory distress syndrome (ARDS), turning the morbidity and mortality rate as high as 14 ~ 40% [26]. When ARDS occurs in patients, the consequences of respiratory failure are obvious as the exchange of oxygen between the lungs and the outside world is restricted and the regulation of blood oxygen is imbalanced. According to statistics, approximately 19% to 70% Txt of patients develop ARDS [2, 36]. The ARDS is a diffuse alveolar injury that can cause increased capillary permeability leading to pneumonia and pulmonary edema, and ultimately to respiratory failure in patients [4, 144]. Therefore, it is particularly important to monitor oxygen saturation at the bedside in patients with polytrauma, especially those with Txt.

1.1.3 Traumatic Hepatic Injury

The liver is the most common type of abdominal trauma. Severe and complex liver injuries (grade III to IV) are likely to be complicated by hemorrhage and shock. The traffic accidents are the main cause of liver trauma, accounting for 49% of cases [16]. The clinical findings of liver trauma are right upper abdominal pain extending to the right shoulder in some cases, hypotension and hemorrhagic shock, and biliary peritonitis accompanied by diffuse pain without intestinal paralysis.

The lacerations with involvement of the hepatic veins are correlated with an increased risk of arterial injury requiring surgical treatment [106]. However, hepatic ischemia-reperfusion injury can occur after surgical resuscitation, especially when surgical control of hemorrhage and repair of liver injury often involves brief blockage of portal flow to control hemorrhage and improve hemodynamics and subsequent reperfusion [91, 108]. Tissue ischemia and hypoxia up to a certain level and time will

lead to cellular damage. Instead of reducing or recovering from the damage, the tissue and cell death are accelerated when the blood is supplied again to the ischemic and hypoxic tissues [49]. This restoration of blood supply to ischemic tissues does not guarantee the restoration of function of the damaged cells, and under certain conditions, it aggravates the damage, which is called ischaemia-reperfusion injury (IRI) [129].

IRI is a dynamic clinical process, and its development and regression can directly affect the choice of clinical treatment. The liver is the largest digestive organ in the body, and it is the center of substance metabolism on the one hand and an important immune organ on the other. A variety of stress hormones, mediators and cytokines produced during traumatic stress can lead to damage and functional changes of hepatocytes through direct or indirect pathways. The damage and functional changes of hepatocytes will definitely affect the stress regulation function of the body. The liver also plays an important role in the occurrence of multi-organ failure, and the changes of liver function will affect the prognosis and regression of the body. Aggravation of liver injury will lead to the occurrence of multi-organ failure [92].

1.1.4 Femoral Fracture

Patients with polytrauma frequently (84.1%) suffer from fractures of the femoral shaft [35, 117]. Although the probability of bilateral femoral fractures in a single trauma is low (1-7%), the mortality rate is high [159]. The main reason behind the high mortality rate is the susceptibility to acute respiratory distress syndrome [104].

The choice of treatment modality for patients with multiple traumatic femoral shaft fractures and the comparison of outcomes has been controversial, with the prevailing view being that there are two modalities, namely external fixation and intramedullary nailing. External fixation is generally used for patients with open fractures. The advantage of this surgical method is that it avoids osteonecrosis due to non-healing of

the wound. If the surgical method of internal fixation is used, it can easily lead to osteomyelitis in the event of wound or inflammatory irritation at the fracture site. The choice of intramedullary nailing for femoral shaft fractures in patients with multiple injuries may lead to a significant increase in inflammatory factors in the postoperative period and a possible 'second insult' phenomenon. The reasons for this phenomenon may be related to the time of surgery, extend of blood loss, vasodilation and the method of intramedullary nail insertion [22, 73]. It is worth noting that patients with multiple fractures of the femur with concurrent hepatic ischaemia-reperfusion injury may release large amounts of inflammatory factors and trigger local and distant inflammatory reactions in the liver due to ischaemia-reperfusion injury [108]. The mechanism by which this inflammatory response affects fracture healing is still unclear. Furthermore, it has been documented that in patients with severe injuries, the inflammatory response progresses due to organ dysfunction and that secondary blows from internal fixation of the fracture can exacerbate the inflammatory response and subsequently lead to ARDS or MOF leading to death [28, 34].

1.1.5 Traumatic Haemorrhagic Shock

Traumatic exsanguination is a common clinical pathological process. When patients are in the traumatic exsanguination condition, their tissue cells are in an oxygen-deprived microenvironment. The resulting microcirculatory disorders are very destructive and can even lead to shock in severe cases [77, 119]. Traumatic haemorrhagic shock refers to the patient's massive blood loss caused by trauma, which leads to ischemia and hypoxia in tissues and organs due to insufficient effective circulation, resulting in metabolic disorders and other pathological changes, eventually leading to MOF [58, 123]. The incidence of MOF is high in cases of severe trauma and remains a major cause of morbidity and mortality (approximately 33%) [99, 141]. Massive bleeding in traumatic patients results in tissue hypoxia which can activate a series of inflammatory factors through hypoxia-inducible transcription

factor (HIF) and other pathways driving inflammation [118, 157]. Inflammation is, on the one hand, the body's defence response to damaging factors. But on the other hand, the inflammatory response itself is a destructive factor to the tissue. The inflammatory response also aggravates tissue hypoxia. Mutually, the damage effect is continuously amplified, which in turn leads to a vicious circle of metabolic acidosis, coagulation disorders, and hypothermia in patients [132]. If this vicious cycle is not intervened in a timely manner, the patient's disease course often deteriorates dramatically or even leads to death.

1.2 Hepatic Response to Major Trauma

1.2.1 Pathophysiological Changes

It is known that 5-10% of patients with severe liver injury or multiple injuries develop liver failure, which is a major cause of death or poor prognosis [170]. The underlying mechanisms involve an altered internal and external cellular environment and a dysregulated perfusion, which in turn lead to barrier failure and apoptosis, and could cause liver dysfunction. Numerous pathological states have been repeated in the context of hepatic ischaemia-reperfusion injury and hepatic excisional injury [90, 125]. It is therefore particularly important to dynamically monitor liver function following trauma in a timely manner. Commonly used clinical measurements currently include the liver transaminases alanine aminotransferase (AST), aspartate aminotransferase (ALT) and alkaline phosphatase (ALP). Patients in shock can develop dramatic increase in blood levels of AST and ALT in the liver (up to 20 times the normal level) which is also called ischaemic hepatitis [126]. The markers AST and ALT were originally defined as indicators of liver damage [41, 62]. AST is widely distributed throughout the organism. It is not only found in the cytoplasm and mitochondria of hepatocytes, but also in the cardiac muscle, skeletal muscle and the brain. Therefore, it lacks specificity as a marker of liver damage. In humans, ALT1 is

found in particularly high concentrations in the hepatocyte cytoplasm and ALT2 is expressed at high levels in adipose tissue, the kidney and the brain. Therefore, the ALT1 concentration better reflects hepatocyte damage compared to AST2 [78, 148]. ALP increases when the tubular membrane of hepatocytes is disrupted. It is transferred to the based surface of the hepatocyte with the gap in the tubular membrane and subsequently permeates to the serum and leads to an elevated concentration of ALP being detected [163].

Direct-liver trauma IRI is a common pathophysiologic process in multiple injuries, haemorrhagic shock or major liver surgery [55, 79]. During ischaemia, the first thing that occurs in hepatocytes due to the lack of adequate oxygen supply is a reduction in ATP metabolic activity with increased glycogen consumption. During the subsequent reperfusion phase, oxygen-induced systemic and mitochondrial reactive oxygen species (ROS) production further exacerbates liver injury. Ischemia-induced cellular dysfunction and death also leads to the production of damage-associated molecular patterns (DAMPs), including histones, mitochondrial DNA and High-Mobility-Group-Protein Box 1 (HMGB-1), as well as inflammatory mediators such as IL-6. The liver-system interaction activates the local immune system, including neutrophils, Kupffer cells, dendritic cells, natural killer cells (NK cells), and T cells [146, 150]. Hepatic IRI stimulates the production of chemokines and chemoattractants (such as complement activation products), which further enhances liver immune cell recruitment from the circulation. Besides, assisting in the clearance of damaged and infected cells, immigrated cells can cause host damage and exacerbate IRI, creating a “vicious circle” of liver damage [50, 166]. According to the type of damage they cause to liver cells, IRI associated with the liver can be classified into two categories: 1) warm IRIs, which result from the damage to liver cells following injury or haemorrhage at body temperature (including minor temperature fluctuation); 2) cold IRI, which occurs during cryopreservation of the liver which causes mainly endothelial cell damage and microcirculatory disturbances in the liver sinusoids [38, 54, 166]. The resulting inflammatory immune response can produce

direct or indirect cytotoxic effects in addition to the metabolic changes caused by glycogen consumption, hypoxia, and ATP depletion [166]. IRI of the liver appears to have "holistic" consequences, affecting not only the lungs and kidneys, but also the intestines, adrenals, brain, and many other organs [97]. Hence, the study of how to reduce the damage to the liver itself and other organs after trauma the liver IRI is of great importance to improve the outcome of trauma patients and their prognosis.

1.2.2 Intracellular Calcium Overload

As of now, the exact mechanisms of liver IRI are still unclear [76]. However, it has been found that the onset and development of IRI is associated with calcium overload and the production of ROS [25]. However, intracellular calcium overload appears to have a greater effect on IRI [15]. There are three mechanisms that can be used to maintain the concentration of intracellular Ca^{2+} at relatively low levels under natural physiological conditions: cell membrane selective permeability, ion pumps, and the endoplasmic reticulum. An increase in intracellular calcium ion transfer to the extracellular space during hepatic IRI is caused by a decrease in intracellular adenosine triphosphate (ATP). Furthermore, Ca^{2+} is released from the endoplasmic reticulum [44].

1.2.3 Oxidative Stress Response

Trauma- or shock-induced IRI to the liver manifests as an aseptic inflammatory response. This type of inflammatory response is characterized by excessive production of ROS and is usually accompanied by a predominant activation at the level of the innate immune system [100, 149, 150]. During the early stages of IRI development, the sources of ROS production are hepatic epithelial cells and predominantly Kupffer cells. In the late stage of IRI, migrating, aggregated and activated neutrophils are the main source of ROS production [14]. A wide variety of

enzymatic reactions are also capable of producing ROS in mammals, but four enzymatic systems predominate: nicotinamide adenine dinucleotide phosphate (NADPH) oxidase, xanthine oxidase, nitric oxide (NO) uncoupling synthase, and mitochondrial electron transport chain. After trauma, the amplifying effect of the cascade reaction not only promotes enzyme interactions but also stimulates ROS production and oxidative stress even more [153]. The liver accumulates neutrophils migrating from various parts of the body during the later stages of IRI. As a result of the binding of CD11b/CD18 on neutrophil surfaces to ICAM-1 on hepatocyte surfaces, neutrophils activate NADPH oxidase, which eventually leads to the production of superoxide anion [12, 70, 93]. However, the liver and other organs can be irreversibly damaged and die when ROS levels are high, leading to imbalances in oxidation and antioxidant systems.

1.3 Inflammatory Response

Patients with severe tissue damage, turn the organism vulnerable to DAMPs and hypoxic damage. This is a prerequisite for the development of local and systemic aseptic inflammatory reactions. The ultimate consequence is the massive release of chemokines and cytokines into the blood, which further aggravates the tissue damage [50]. Inflammatory mediators and DAMPs are primarily sensed by pattern recognition receptors (PRRs) [162]. Various PRRs and complement receptors on various cells including hepatocytes transmit the danger signals to intracellular pathways and thereby provide a cellular defence response [50].

1.3.1 Hepatocytes

Several DAMPs, including HMGB1, ATP and mitochondrial DNA, are released by hepatocytes that have been exposed to trauma or stress [71], bind to PRRs such as toll-like receptors (TLRs) in the cytoplasm or on cell surfaces [1, 63]. A range of TLRs expressed by hepatocytes exert powerful immune effects against DAMPs and other early deleterious factors [81, 142]. Both hepatocytes and Kupffer cells express

TLR2,3,4, with the difference that hepatocytes express TLR5 and Kupffer cells express TLR9 [17]. Interestingly, TLR acts as an immunosurveillance receptor, but nevertheless may contribute to tissue damage during IRI by enhancing the inflammatory response and further exacerbating it [60, 75]. Of note, Although the small amount of ROS produced by the hepatocytes themselves does not cause significant cell damage, these ROS can induce the release of HMGB1 into the blood. HMGB1 binds to TLR4 on the surface of Kupffer cells and induces an inflammatory response leading to the production of more ROS, which may lead to a vicious cycle [14].

1.3.2 Kupffer Cells

For an effective inflammatory response, Kupffer cells (KCs) in the liver are required. They are the largest population of macrophages in the body [110]. KCs are a type of macrophage that serves a defensive purpose by engulfing tissue debris after trauma. However, in the early stages of reperfusion, activated KCs can produce ROS and pro-inflammatory factors including tumour necrosis factor (TNF)-α, IL-1β, IL-2, IL-6, IL-10, IL-12 and IL-18 [14, 23, 136] (Figure 1). The cascade of TNF-α and other inflammation mediators is critical in contributing to the development of liver injury. TNF-α recognises and binds to receptors on the surface of hepatocytes, thereby activating nuclear factor-κB (NF-κB) and mitogen-activated protein kinase (MAPK), leading to liver damage [1]. TNF-α secreted by KCs further promotes the recruitment and aggregation of inflammatory cells by upregulating the expression of ICAM-1 and vascular cell adhesion molecule (VCAM)-1 [56]. In addition, necrotic KCs can also secrete HMGB1, which acts as a strong DAMP and induces strong inflammatory signals [147]. There is a persistent trend towards increased levels of HMGB1 in the liver in the 24 hours following trauma [68]. Activated KCs damage hepatocytes and sinusoidal endothelial cells, ultimately resulting in necrosis of the hepatocytes [21].

1.3.3 Neutrophils

When the body suffers trauma or is in ischaemic decompensation, the neutrophils that migrate from the blood vessels into the liver remove tissue debris but also can damage the hepatocytes in different ways [1]. It is the damaged mitochondria and activated complement that activate neutrophils after trauma. The damaged mitochondria secrete large amounts of DAMPs, while complement activation produces anaphylatoxins. Both are jointly involved in the activation of neutrophils [51, 167]. Activation of neutrophils results in their massive accumulation in the liver and the consequent increase in liver levels of CD11a/CD18 (LFA-1) and CD11b/CD18 (Mac-1). The increased LFA-1 and Mac-1 appeal to ICAMs and attach themselves to the liver endothelium. In turn, neutrophils migrate along a gradient of chemoattractant activity, like anaphylatoxins and macrophage inflammatory protein-2 (MIP-2) [57]. The ROS released by neutrophils passing through the liver sinusoids and accumulating in the liver tissue interstitium also damage the liver tissue [94, 160, 164]. At later stages of IRI progression, various proteases released by neutrophils, including collagenases, elastase, and cathepsin G, may further damage the hepatocytes [85, 111] (Fig 1)

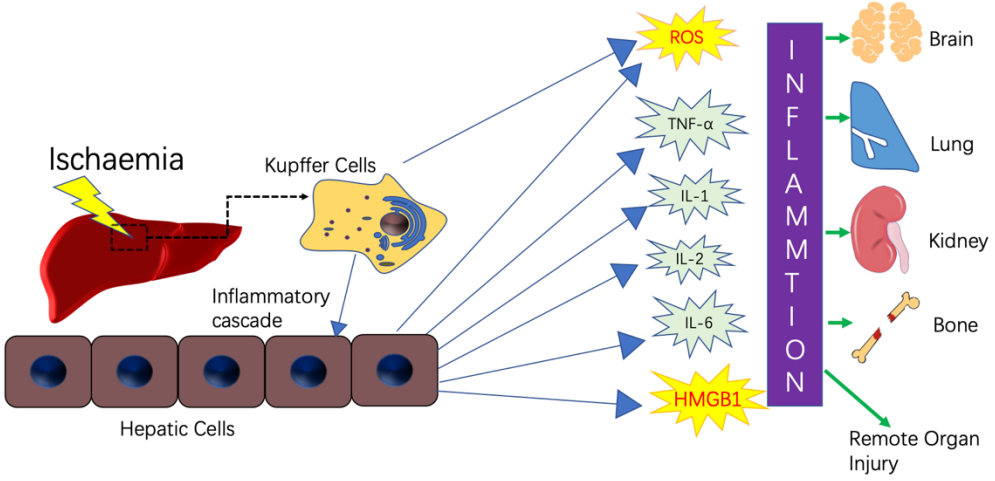

Figure 1: Immune response induced by IRI due to multiple injuries and haemorrhagic shock. Trauma-induced IRI damage causes activation, apoptosis and necrosis in hepatocytes, Large amounts of inflammatory factors such as High-Mobility-Group-Protein Box 1 (HMGB1), reactive oxygen species (ROS) and

interleukins cross the Disse Space and enter the bloodstream to participate in the inflammatory response, causing tissue fibrous alteration. Activated hepatocytes themselves can also produce numerous inflammatory mediators, such as complement component 1r (C1r), which can also participate in the local or systemic inflammatory response [43, 128, 169]. The inflammatory mediators released into the bloodstream not only damage the liver cells themselves, but also distal organs such as the brain, lungs and bones. Image was made by powerpointr.

1.4 Liver as the primarily damaged organ

Cytokines and inflammatory mediators released by Kupffer cells in IRI are a principal source of systemic inflammatory cascade multiplication, as demonstrated in a model of liver transplantation-induced IRI [30]. Although the mechanisms of activation of the inflammatory response by DAMPs and related inflammatory mediators remain unclear, it is generally accepted that PRRs receive inflammatory signals from DAMPs and induce the development of SIRS. After the occurrence of SIRS, the distal brain, lung and kidney are affected at varying degrees due to the “cytokine storm”, clinically manifesting as a multi-organ dysfunction syndrome [57, 139]. The liver, as the largest metabolic organ in the body, is also the central target organ for the systemic inflammatory response attack in this systemic storm of inflammation [88]. Moreover, a dramatic alteration in the transcriptome of extrahepatic organs suggests that the serum metabolite-mediated crosstalk between the liver and extrahepatic organs contributes significantly [168].

Fractures of the pelvis and femur can lead to traumatic haemorrhagic shock in a short period of time with blood loss exceeding 500 ml or more, leading to severe liver IRI and subsequent aseptic inflammation. However, bone formation and bone repair cannot be achieved without various growth factors. The liver is involved in bone metabolism through the regulation of parathyroid hormone (PTH) and the synthesis of growth factors such as insulin-like growth factor (IGF)-I and IGF-II [19, 66]. PTH regulates calcium and phosphorus metabolism in vertebrates, increasing blood calcium levels, decreasing blood phosphorus levels and inducing liver production of IL-6 to affect bone metabolism [86]. Moreover, it can increase the activity of various

bone molecules, shorten the half-life of bone factors, and affect their circulation levels in the body [95]. Haemorrhagic shock caused by multiple fractures often leads to hepatic IRI [151]. Lack of timely and effective treatment after trauma is an important factor contributing to liver damage and many therapy also affect fracture healing. Some clinical studies have demonstrated significant inflammatory factor activity in the liver 1h after trauma, while AST peaks 5h after trauma [69]. Inflammatory factors released from femoral fractures interact with inflammatory factors released from hepatic IRI, but the mechanisms regarding the impact on fracture healing remain unclear. Although it has been suggested that both local inflammation and systemic influence can impair fracture healing, the mechanism of action still requires further study [9, 48, 168]. For this reason, further investigation are required to define how inflammatory factors produced after liver injury affect fracture healing and what effective interventions are available.

1.5 Aim of the Study

Bilateral femoral shaft fractures combined with ischemia-reperfusion liver injury represent a critical state of neurological and humoral regulation. Thus, there are serval questions to be addressed: What are the changes in liver function during bilateral femoral fractures combined with ischemia-reperfusion liver injury in the setting of multiple injuries? Do the changes in liver function affect the healing of the fracture? It is important to discuss these questions for the proper management of multiple trauma: How to apply appropriate immunotherapy to avoid aggravating the existing organ damage?

The ischemic tolerance of the liver to trauma in the setting of polytrauma with combined pulmonary contusion, hepatic dissection, and bilateral femoral shaft fractures is uncertain. The contribution of various cytokines released after liver injury to the liver itself and distal organs still needs to be explored.

Therefore, we hypothesized that experimental polytrauma results in an alteration of liver mediators relevant for inflammation and bone fracture repair; and furthermore, that this response is improved by an immunomodulation approach targeting complement factor C5 and TLR-coreceptor CD14.

2. Material and Methods

2.1 Animals

In this study, all experiments were carried out in accordance with German Animal Research Legislation and in compliance with the "Principles for the Care of Laboratory Animals". The official permission was granted by the Office for Nature, Environment and Consumer Protection of the State of North Rhine-Westphalia (the State Agency for Nature, Environment and Consumer Protection North Rhine-Westphalia (LANUV), the official number was AZ 81-02.04. 2020.A215. The Office for Nature also approved all experimental protocols. Male pigs (German Landrace) aged between 12 and 16 weeks (weight 35±5 kg) were kept on a 12-hour day/night rhythm for 7 days prior to the experiment to acclimatize to their surroundings. Before the start of the experiment, all animals were provided by a disease-free breeding facility, and examined by a veterinarian upon delivery.

All data presented in the paper were collected in the context of a larger study in order to benefit from the 3R (replacement, refinement, and reduction) principle.

2.2 Instruments

0.2 mL Thermo - Strip	Thermo ScientificTM, USA
1 mL syringe	BD Biosciences, USA
10mL syringe	BD Biosciences, USA
50 mL syringe	BD Biosciences, USA
96-well microtiter plate	Thermo ScientificTM, USA
96-well plate	Thermo Scientific, USA

Animal lancet	Paul Danz, Germany
Arterial line	Vygon, Germany
Biopsy and embedding cassettes	VWR Histosette, Germany
Bolt gun machine	Blitz-Kerner, turbocut JOBB GmbH, Germany
Cannula 30G	Braun Melsungen, Germany
Cattle-killing cartridges	DynamitNobel AG, Troisdorf, Germany
Central venous line	Teleflex Medical, Germany
Centrifugation concentrator	Sartorius, Germany
Cover slips	Menzel GmbH, Germany
Cytoside	Fisher Scientific, USA
Cytoside shandon filter card	Fisher Scientific, USA
Disposable weighing dishes	VWR Histosette, Germany
EDTA microtube	Monovette, Germany
Eppendorf reaction tube 0.5 mL	Eppendorf, Germany
Eppendorf reaction tube 1.5 mL	Eppendorf, Germany
Eppendorf reaction tube 2.0 mL	Eppendorf, Germany
External fixation (Radiolucent Fixator)	Orthofix, USA
Falcon 15ml tube	BD Biosciences, USA
Falcon 50ml tube	BD Biosciences, USA
Intramedullary nailing	Stryker, Duisburg, Germany
Non-woven compresses	Goldenrod, USA
Orotracheal intubation	Hi-Lo LanzTM, ConsuMed, Germany
Pipette reservoir	Biozym Scientific, Germany
Pipette tip 0,1 - 1 µL with filter	Brand Germany

Pipette tip 0,5-10 µl	Sarstedt, Germany
Pipette tip 0.5-10 µL with filter	Sarstedt, Germany
Pipette tip 10-200 µL	Sarstedt, Germany
Pipette tip 10-200 µL with filter	Sarstedt, Germany
Pipette tip 10-300 µL	Sarstedt, Germany
Pipette tip 100-1000 µL	Sarstedt, Germany
Pipette tip 100-1250 mL with filter	Sarstedt, Germany
QIAshredder™	Qiagen, Germany
QubitTM assay tube	Invitrogen, USA
RNase Zap™	Sigma – Aldrich, Germany
Screw tube	Sarstedt, Germany
Sealing strips for 96-well PCR plate	Thermo Scientific, USA
Surgical Disposable Scalpel	Braun Melsungen, Germany
Three-lumen haemodialysis catheter	Teleflex Medical, Germany
Ultracentrifuge tube	Beckman Coulter, USA

2.3 Machines

Automated chemistry analyser	Ortho-Clinical Diagnostics, USA
Automated haematology analyser	Nihon Kohden, Japan
Automatic pipette	Brand, Germany
Balance M-power	Sartorius, Germany
Centrifuge Fresco 21	Thermo Scientific, USA
Centrifuge Maxifuge 3SR+	Thermo Scientific, USA

Cuntura razor	Wella, Germany
Fluorometer	Invitrogen AG, USA
Freezer -20°C	Bosch, Germany
Freezer -80°C	Thermo Fisher Scientific, USA
Homogeniser Ultra-Turrax T25	IKA Werke, Germany
Intraoperative animal warming system	Föhr Medical Instruments, Germany
Light microscope: Zeiss Axio Imager	Carl Zeiss, Germany
Microscope “CK2”	Olympus, Japan
Microtome slee cut 6062	SLEE medical, Germany
Multichannel pipette 20-200µl	VWR International, USA
Multichannel pipette 5-50µl	VWR International, USA
Multichannel pipette 50-300µl	VWR International, USA
Multipette plus	Eppendorf, Germany
Pipetboy accu	Integra biosciences, Germany
QIAshredder homogenizer	Qiagen, Germany
Recording monitor LCD TFT	Dell, USA
Tecan Sunrise Plate Reader	Tecan, Switzerland
Thermal cycler	Stratagene, USA
Transferpette S 1000µl	Brand, Germany
Transferpette S 100µl	Brand, Germany
Transferpette S 10µl	Brand, Germany
Transferpette S 200µl	Brand, Germany
Transferpette S 20µl	Brand, Germany
Ultrasonic homogeniser UW 2070	BANDELIN, Germany

Vortex Genie 2	Scientific Industries, USA

2.4 Kits and regents

AffinityScript cDNA Synthesis Kit	Agilent Technologies, USA
ALP primer	Biomer.net, Germany
Bicinchoninic Acid Protein Assay Kit	Thermo Scientific, USA
cDNA Synthesis Kit	Agilent Technologies, USA
Dako REALTM Detection System	Agilent Technologies, USA
Housekeeping Gene (GADPH)	Biomer.net, Germany
IL-10 primer	Biomer.net, Germany
IL-2 primer	Biomer.net, Germany
IL-6 primer	Biomer.net, Germany
MPO antibody	Abcam, Germany
OCN primer	Biomer.net, Germany
OPG primer	Biomer.net, Germany
OPN primer	Biomer.net, Germany
Pig OPG ELISA Kit	Lsbio, USA
Porcine RANK ELISA Kit	Mybiosource, USA
Porcine RANKL ELISA Kit	Mybiosource,USA
RANK primer	Biomer.net, Germany
RANKL primer	Biomer.net, Germany
RNase - free DNase - set	Qiagen, Germany
RNeasy® Mini Kit	Qiagen, Germany
TGF-β primer	Biomer.net, Germany

TLR4 primer	Biomer.net, Germany

2.5 Reagents , Buffer and Chemicals

Aqua Ampuwa rinsing solution	Fresenius Kabi, Germany
Azaperone	Elanco, USA
Bovine serum albumin (BSA)	Sigma – Aldrich, Germany
Crystalloid infusion	Sterofundin® ISO, Germany
Diethyl pyrocarbonate (DEPC)	Ambion, USA
DPBS (1X) without Ca^{2+} & Mg^{2+}	Thermo Scientific, USA
EDTA-free protease inhibitor mix	Roche, Germany
Ethanol pure	Sigma – Aldrich, Germany
Ethylenediaminetetraacetic acid	Lonza, Switzerland
Fentanyl 0.5mg/10ml	Rotexmedica, Germany
Formaldehyde - solution	Fischar, Germany
Haematoxylin solution	Sigma – Aldrich, Germany
Midazolam 5mg/ml	Rotexmedica, Germany
NaCl 0.9%	Fresenius Kabi, Germany
Neo-Mount	Sigma – Aldrich, Germany
Norepinephrine 1mg/ml	Arterenol, Germany
Paraffin	McCormick, Germany
Pentobarbital	Narcoren, Germany
Potassium chloride	Pascoe, Germany
Propofol 1%	Fresenius Kabi, Germany

Protease inhibitor cocktail P8340	Sigma Life Sciences, USA
Tetramethylbenzidine (TMB)	LSBio, USA
TMB Substrate Reagent Set	LSBio, USA
Tissue-Tek OCT embedding solution	Sakura Finetek, USA
TRIS - EDTA buffer solution	Thermo Scientific, USA
Tris-buffered saline (TBS)	Sigma – Aldrich, Germany
Tween 20	Sigma – Aldrich, Germany
Xylene	VWR International, USA
β- Mercaptoethanol	Sigma – Aldrich, Germany

2.6 Software and Tool

Software applied for the experiment is enumerated as follows:

BioRender

GraphPad Prism 7

ImageJ 2018

Microsoft Office 2016

SigmaPlot 11.0

Zeiss AxioVision SE64 Rel. 4.9

2.7 Methods

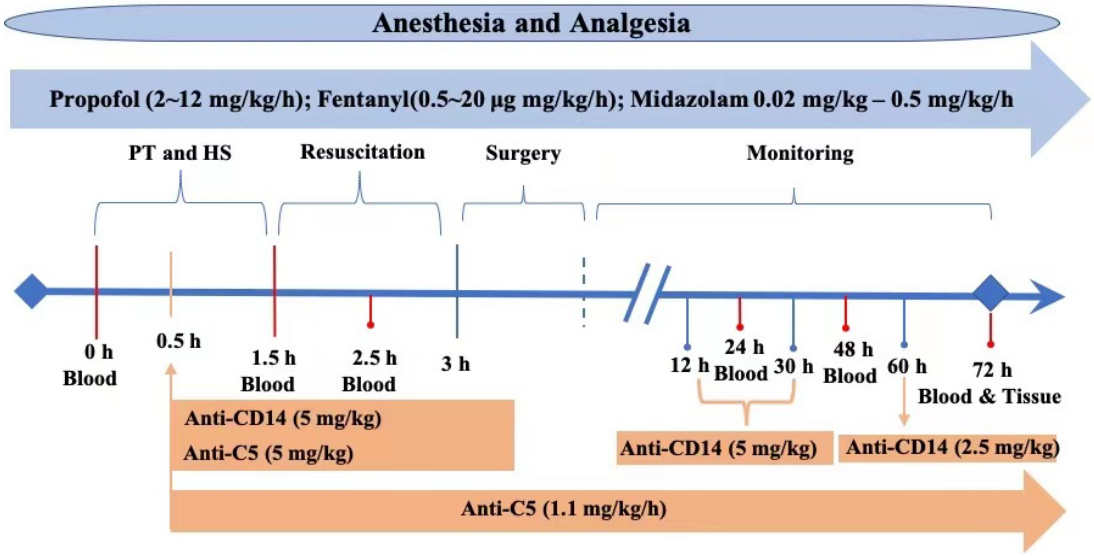

Figure 2: Trauma modelling. The pig experiments were performed at the RWTH Aachen. Anesthesia and analgesia was applied during the whole expected course. Polytrauma included liver injury, blunt chest injury, femoral fracture and haemorrhagic shock. Blood samples were taken at 0 h, 1.5 h, 2.5 h, 24 h, and 48 h after the model was established, and blood and other tissue samples were taken at 72 h. A bolus of C5 inhibitor (5 mg/kg) 30 min post-trauma with a subsequent continuous infusion (1.1 mg/kg/h) until 72 h after the trauma, and anti-CD14 inhibitor boluses of 5 mg/kg at 30 min, 12 h, and 30 h and of 2.5 mg/kg at 60 h post-trauma. C5 = Complement 5. CD14 = Cluster of differentiation 14. Image prepared by self.

2.7.1 Preoperative preparation

Premedication was performed by intramuscular injection of azaperone (4 mg/kg BW). Intraoperative anaesthesia was routinely induced and maintained with Propofol, Fentanyl, and Midazolam. Then, a mechanical ventilation was allowed by placing a tracheal intubation. All drugs were administered through a central venous line to the animals. Next, the animals were maintained on ventilation using a closed anaesthesia device. The flow-controlled mode was used to ensure a pressure limit of Pinsp of 30 cm H_2O and lung-protective tidal volumes, achieving a $PaCO_2$ ranging from 35-45 mm Hg. In order to establish a haemorrhagic shock model at a later stage, a dialysis catheter was inserted into the left femoral vein of the animal. To detect blood pressure fluctuations, an arterial catheter was positioned in the left femoral artery. In addition, the urinary bladder was catheterised via a suprapubic catheter using a

mini-laparotomy. The animal's vital signs were continuously observed for stability during the establishment of the trauma model, and the time taken to establish this process generally took 3-4 hours. When the animal's vital sign values were stable, the animal's body temperature was raised by a blower and the animal was covered with a blanket. The target body temperature was 38.5 ± 0.5 °C. Furthermore, the simulated surrounding during the trauma period was a 21% oxygen environment, which means that trauma was induced in a standard air condition. In order to support stabilization and ventilation of the pigs, the animals were turned every 4-6 hours.

2.7.2 Trauma modelling and 72 h ICU standard care period

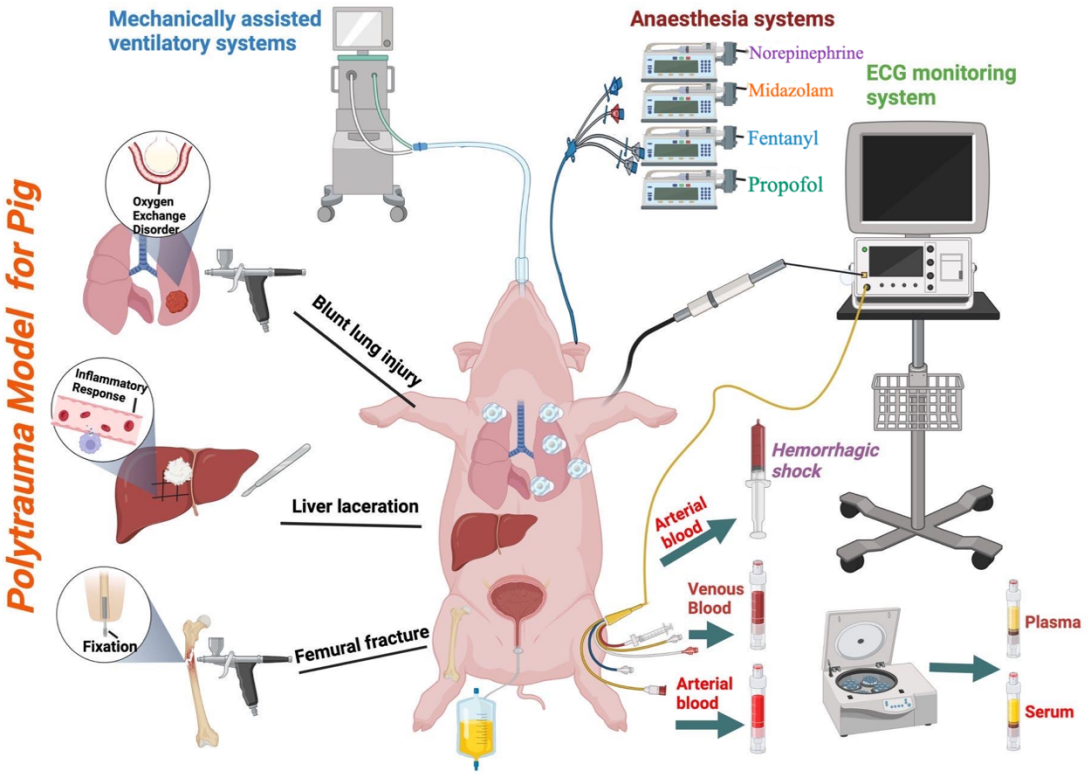

Figure 3: Schematic diagram of the pig trauma model. The pigs were subjected to blunt thoracic contusions, liver laceration, and femur fractures of both lower limbs respectively. The vital signs of the pigs were dynamically monitored to simulate an ICU environment. ECG = Electrocardiography. Image made by self.

2.7.2.1 Haemorrhagic Shock

All experimental animals were strictly monitored for vital signs throughout the experiment, especially after finishing the haemorrhagic shock. The haemorrhagic

shock was induced as follows. A double-lumen haemodialysis catheter was inserted into the right femoral artery and left femoral vein of the animal under aseptic manipulation and the animals' arterial pulse was monitored. The animals' blood pressure, mean arterial pressure, pulse and heart rate were closely monitored by Pulsion Medical's sphygmomanometer. Haemorrhagic shock was induced by drawing venous blood from the left femoral vein under pressure control and volume limitation, with a targeted mean arterial pressure of 40 ± 5 mmHg. In general, it was necessary to withdraw 45% of the total blood volume. The withdrawn blood was saved in blood bags for reperfusion inducing induction of reperfusion injury. The total course of haemorrhagic shock was maintained for 90 min. After 90 min, the intake of crystalloid solution is promptly injected or reduced according to the changes in the animals' blood pressure.

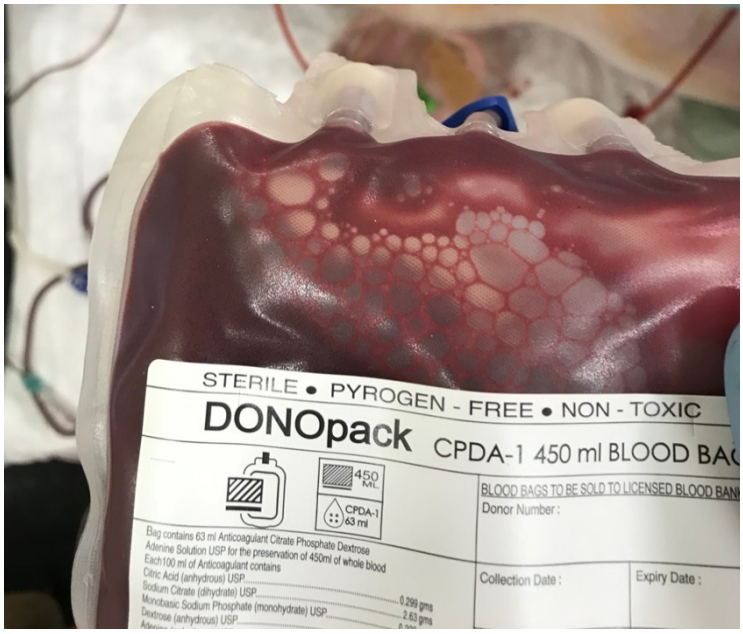

Figure 4: Haemorrhagic shock models. All operations were carried out in a sterile environment and all blood drawn was returned to the animal after 90 min. To prevent hypothermia, we maintained the body temperature (38.5±0.5 °C) with the WarmTouch® thermal system. Image obtained from Johannes Greven's laboratory.

2.7.2.2 Blunt Chest Trauma

The animal was kept in the right lateral recumbent position. The standardised chest trauma was induced with the bolt gun during inspiration. This created an isolated, unilateral, blunt chest trauma with a lung contusion in the area of the lower and middle lobe. A pair of Panels were placed (steel: 0.8 cm and lead: 1.0 cm thick) on the dorsal side of the right chest, inferior to the thorax. Setting a bullet through a cattle-killing gunshot in this panel induced the blunt chest trauma.

2.7.2.3 Traumatic Liver Injury

The animals were placed in the supine position on the operation table. The upper abdomen was disinfected with an iodophor, and the upper abdomen was dissected to enter the abdominal cavity. A transverse wound (4.5 cm * 4.5 cm) was made in the middle lobe of the liver to a depth of half the thickness of the liver, allowing uncontrolled bleeding for up to 30 seconds. The liver was then wrapped in 10*10cm gauze to close the open procedure.

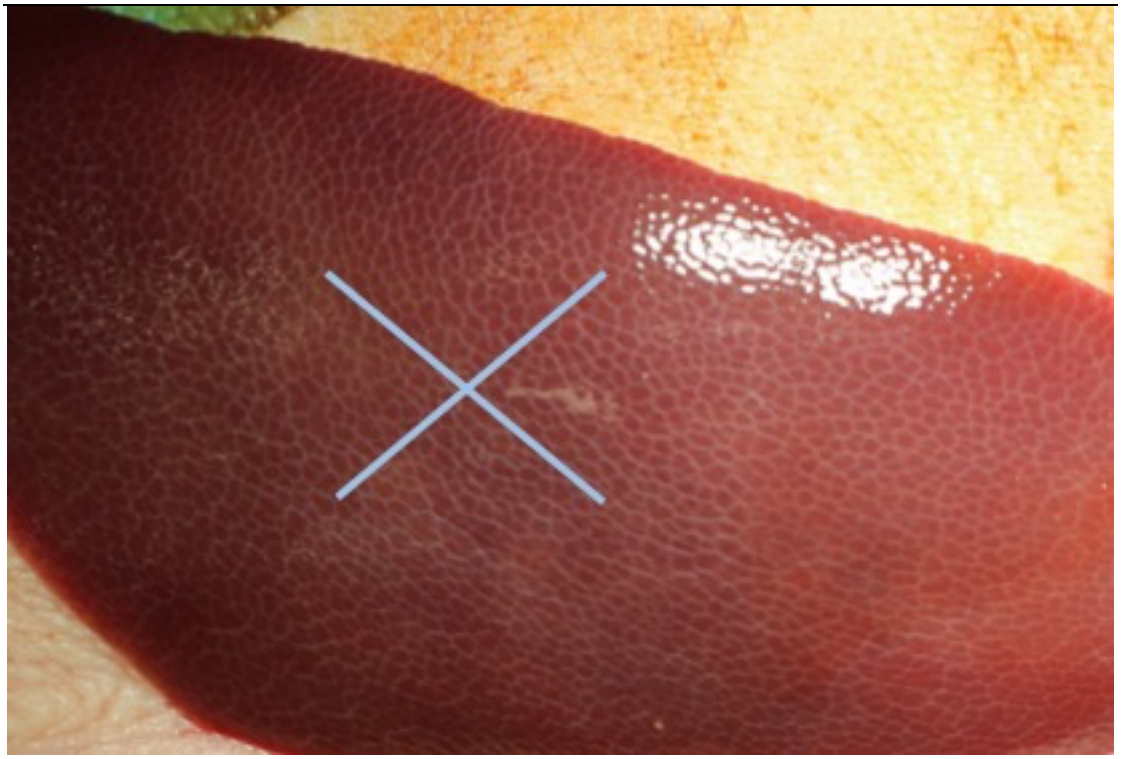

Figure 5: Liver trauma model. After a laparotomy and advancement of the liver, a crosswise incision of the left liver lobe (4.5 cm * 4.5 cm) was made, which induced uncontrolled bleeding that was not treated in around 30 seconds. The escaping blood was collected with pre- and posttraumatic weighed abdominal cloths. Next, the abdomen was tamponaded around the resected liver with abdominal drapes (liver packing). The abdomen was then closed. Wound control and dressing changes were performed daily. Image obtained from Johannes Greven's laboratory.

2.7.2.4 Femoral fracture

The animal was placed in a supine position, and the skin area of the femur and groin was routinely disinfected with iodophor. The target lower limb was immobilized, and the limb on the side to be injured was placed in a mildly externally rotated position. A longitudinal surgical incision of approximately 3 cm in length was made in the femoral shaft, a T-shaped metal plate was placed on the middle third of the femoral shaft, and the T-shaped plate was fired with a bolt gun mechanism and a bull killing bullet. The impact was made through the bullet to the T-plate impacting the middle femur.

2.7.2.5 Experimental Groups

A total of 25 animals were included in this experimental study. Femoral fracture repositioning and fixation were performed by a senior surgeon at the RWTH Aachen University Hospital and the rest were responsible for the auxiliary work. We performed surgical sterilization and aseptic sheeting of the limb on the prepared treatment side again after the animals were resuscitated and the femoral fracture was surgically stabilized. The fractures were treated using either external or internal fixation according to the protocol. Eight animals supported with intramedullary nailing (one animal died during the establishment of a multiple injury model) were in the Nail group, and eight animals treated clinically with an external fixation system were in the Fix ex group. To facilitate comparative studies, we selected 6 non-injured animals receiving the same instrumentation, drugs, and treatment regimen, but without trauma intervention, as the Sham group. Finally, a group objected to the multiple injury models followed by treatment with an intramedullary nailing received a simultaneous intravenous infusion of C5 inhibitor and CD14 inhibitor immunotherapy named the Nail+Therapy group. The C5 inhibitor we used is RA101295 (2-kDa peptide), which was provided by UCB Pharma (Brussels, Belgium). rMil2 applied on the animal as recombinant anti-porcine CD14 antibody (clone MIL2; isotype IgG2a), made recombinant as an IgG2/4 chimera from the laboratory of Professor T.E. Mollnes (Norway). We gave antibiotics intravenously to all animals at 24-hour intervals after the trauma model was completed until the end of the experiment.

2.7.2.6 Surgical techniques

After the completion of the bilateral closed femoral fracture model, either external fixation treatment method or internal fixation treatment method with intramedullary nailing were applied to both lower limbs of the same animal.

A: Intramedullary nailing treatment.

The pig was placed lateral decubitus on the operating table and the incision site was disinfected with iodophor. A lateral incision of the left lower limb of the pig was first performed, about 5 cm long, and the skin and subcutaneous tissue were incised layer by layer. The lateral bone muscle was separated and distracted to expose and reposition the fractured bone. The entry point of the intramedullary nail was located at the knee level. This point was first drilled with an electric drill to open the medullary canal, and the guide pin was driven from the distal fracture end to the proximal fracture end. The intramedullary nail was placed using the guide pin. Afterwards, the guide pin was removed and the nail fixed with 4 screws in total (2 at the proximal end and 2 at the distal end). After the intramedullary nail was placed, the skin incisions were sutured.

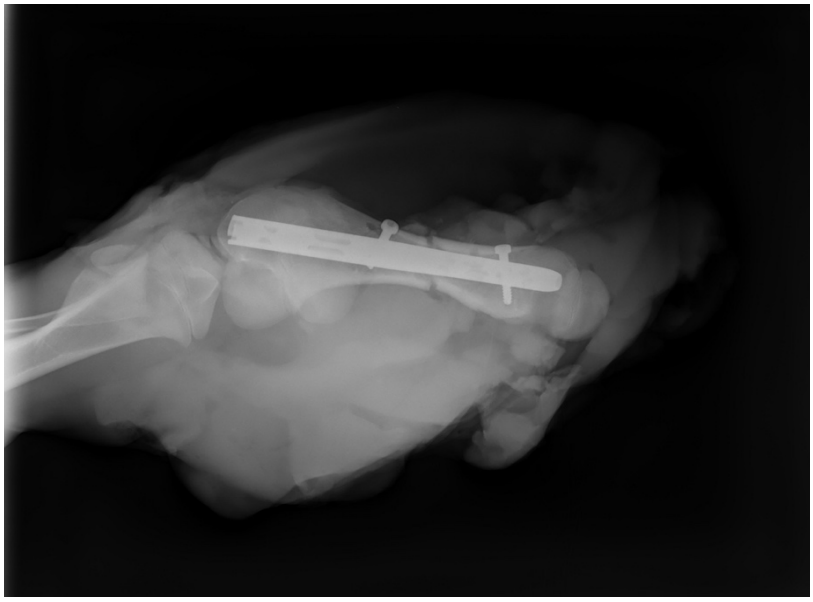

Figure 6: Radiographs of femoral shaft fractures treated by internal fixation (Stryker, Duisburg, Germany). It is clear from the radiograph that the fracture line in the middle of the femur fracture is clearly visible. The fracture end is well reposed and there is no damage to the rest of the bones. The intramedullary nail is fixed in place and there are no artefacts such as free fracture fragments, indicating that the fracture model and comesponding treatment was successfully performed. Image obtained from Johannes Greven's laboratory.

B: External fixation.

The experimental animals were placed in the lateral decubitus. The right lower limb and its groin and other surgical areas were disinfected with iodophor and aseptically sheeted. A longitudinal incision of about 4 cm was made on the anterolateral side of

the right lower limb, the skin and subcutaneous fascia were incised, and the muscles were bluntly separated to expose the fracture line. The soft tissue was removed, and the fracture was repositioned using a bone holder. From the anterolateral side of the incision, a pin entry point was selected and 4 small longitudinal incisions of approximately 0.6 cm were made for the pin placement (2 at the proximal end and 2 at the distal end). After drilling the holes, 4 pins and external fixation brackets were attached, and the brackets were subsequently adjusted and fixed.

Figure 7: External fixation for femoral shaft fracture. The external fixation brace T2 system for femoral fractures was used. The warmed dressing at the wound was closely monitored during the simulated ICU surveillance. Image obtained from Johannes Greven's laboratory.

2.7.3 Blood Sampling

The blood samples used in the study were obtained after resuscitation and surgical treatment (0 h) and at 1.5 h, 2.5 h, 24 h, 48 h, and 72 h afterwards. Subsequently, after centrifugation at 2000 x g for 15 min at 4 °C, serum and plasma samples were transferred to liquid nitrogen or stored in a -80 °C freezer for subsequent experiments. At the end of the observation period, animals were given 20 ml Narcoren® (1ml Narcoren® corresponds to 160 mg pentobarbital) intravenously and then the animals were euthanised i.v. using 40 ml 1-M potassium chloride, i.e., 1.14-1.33 ml/kg/bw (1ml potassium chloride corresponds to 74.5 mg potassium chloride). The whole blood was collected in sterile plasma EDTA microtube (Monovette®). Then, 10% EDTA-free protease inhibitor mix (Roche) were added and incubated for 10 min on ice. After centrifugation for 10 min at 4000 rpm and 4 °C, the plasma was snap frozen in liquid nitrogen and stored at -80 °C.

2.7.4 Liver Sampling

Samples were taken from the left lobe of the untraumatized liver and cut into 1.5 cm*1.5 cm size samples. One portion was placed in an embedding cassette and subsequently transferred to a formalin solution for fixation (24 h). In addition, the other part of the sample was immediately placed in Tissue-Tek OCT embedding solution, quickly frozen on the dry ice, and stored in a -80 °C freezer until sectioning. Finally, the samples of the left liver lobe were obtained and divided into 1 cm*1 cm size to transfer into Eppendorf reaction tubes. Three samples were placed in each tube and rapidly cooled by liquid nitrogen and stored these samples in the -80 °C freezer.

2.7.5 Analysis of liver damage marker

An automated biochemical analyser (VITROS 350; Ortho-Clinical Diagnostics, Raritan, NJ, USA) of the clinical chemistry laboratory of the RWTH Aachen University Hospital was used for the analysis of ALP, ALT, and AST. The levels of Protein, ALP, ALT, and AST in the whole blood of different time points (0 h, 1, 5 h, 2.5 h, 24 h, 48 h and 72 h after the onset of trauma) were quantified by the automated biochemical analyser.

2.7.6 Histological analysis

Haematoxylin-Eosin staining

To compare the liver injury in different groups, we prepared paraffin sections of individual liver tissue samples and the performed experimental staining of the tissue sections using haematoxylin-eosin (HE) staining.

Liver tissues were well soaked in 10% neutral phosphate-buffered formalin solution. It was dehydrated by gradient concentration ethanol and treated with xylene solution for transparency. The processed samples were embedded in hot-melted paraffin wax. The tissue slides were dewaxed and hydrated before HE staining. Subsequently, they were stained sequentially with haematoxylin, 1% hydrochloric acid ethanol fractionation and weak alkaline aqueous solution. Finally, the sections were immersed in eosin staining solution to complete the staining.

For long-term preservation of the samples, the stained sections were dehydrated by ethanol and transparently treated with xylene. Finally, the sections were sealed with neutral resin, and the histomorphology was observed under the microscope on the next day and the damage scoring was completed.

Scoring

Each sample was observed under the microscope, and the samples were assessed with HE staining. Ten different fields of view were taken under light microscopy to observe erythrocyte sludges, vacuole formation, necrosis (loss of cytoplasmic staining, nuclear consolidation, nuclear lysis and nuclear disappearance) and inflammatory cell invasion (neutrophils) in the liver tissue. Criteria: 0: no necrosis, no bruising and no hepatocyte vacuolation; 1. very slight bruising and fine vacuolation (< 10%), occasional single cell necrosis; 2: mild bruising and vacuolation (11%-30%), mild tissue necrosis (< 30%); 3: moderate to severe bruising, vacuolation and tissue necrosis (31%-60%).The level of inflammation in each group according to the number of neutrophils. No neutrophils in the visual field represented a score of 0, between 1 and 2 neutrophils expressed a score of 1, 3-4 neutrophils stated a score of 2, to have 5-6 neutrophils indicated a score of 3 and over 6 neutrophils denoted a score of 4.

Table 1: Liver score (at x400 magnification). None (extent＜ 0%) for 0 point; mild (extent: 1%~30%) for 1 point; moderate (extent: 31%~60%) for 2 points; serve (extent:＞60%) for 3 points. RBC = red blood cell.

Visual field	Field	1	2	3	4	5	6	7	8	9	10	Average point
Congestion + Red Blood Count (RBC)	Points											
Vacuolization	Points											
Necrosis	Points											
Inflammation (PMN)	Points											
Average point												

2.7.7 Real-time quantitative polymerase chain reaction (RT-qPCR)

A. Extraction of ribonucleic acid (RNA)

We added 600 µl of working solution (10 µl of β-mercaptoethanol per 1 ml of Buffer RLT) to each 1.5 ml sample tube containing tissue fragments. Then the homogenized samples were transferred from all the Eppendorf reaction tubes (2 ml) to QIAshredder tubes using a pipette. Then the samples were centrifugated at 21,000 g (max speed) for 2 min and the suspension was aspirated carefully into Microtube tubes (2 ml). Then we added 600 µl of 70% ethanol to each tube and mix thoroughly. After that, 700 µl of the homogenate was transferred to a RNeasy tube and centrifuged at 8000x g for 15 s. After transferring to a RNeasy tube, 350 µl of Buffer RW1 was added to the tube and continued to centrifuge at 8000xg for 15 s. Then the filtrate was discarded. Mixed 70 µl of buffer RDD solution with 10 µl of DNase I stock solution, noted as D solution. By withdrawing 80 µl of D solution into the RNeasy and allowing the mixture to react for 15 min on the bench. 350 µl of Buffer RW1 was absorbed into the RNeasy tube and centrifuged at 8000 g for 15 s, then the filtrate was discarded in the collection tube. The procedure was repeated three times. Following centrifugation at maximum speed for 1 min, sample RNA was extracted by applying 50 µl of RNase-free water to the RNeasy tube and centrifuging at 8000 g for 1 minute.

The RNA concentration was measured by pipetting 1µl of RNA sample into the working solution with an RNA concentration detector. If the concentration was less than 100 µl/ml the sample was extracted again. Lastly, all samples were stored in a -80 °C freezer.

B. Synthesis of cDNA

Table 2: Number of individual reagents required for each sample. µl=microliter.

Component	**Volume (µl)**
2x First strand master mix	10
Oligo (dT) primer	3
AffinityScript RT/RNase Block enzyme mixture	1
RNA	6
Total volume	**20**

We used a cDNA synthesis kit to reverse transcribe the isolated RNA to cDNA. The process of synthesis of cDNA was as follows:

We prepared a master mix in a 1.5ml Eppendorf reaction tube containing 10 µl of first strand master mix (2x), 3 µl of oligo (dT) primer, and 1µl of AffinityScript reverse transcriptase (RT)/ RNase blocking enzyme mixture for each sample. Then we used a fluorometer to determine the RNA-concentration and the required DNA was calculated to 6 µL. Next a required volume of RNA and 14µL of prepared Master Mix for each sample was then added to 0.2 mL Thermo - Strips. An automatic thermocycler was used to synthesize cDNA from Thermo-Strips with the help of a 96-well PCR plate sealer. The cDNA obtained was diluted with diethyl pyrocarbonate (DEPC)-treated water at a ratio of 1:2 and stored the cDNA at -20 °C for further use.

C. Operation of qPCR

The qPCR was performed using Brilliant III Ultra - Fast SYBR® Green Master Mix.

For each qPCR running, a layout for the 96-well plate was prepared, and the amount of Master Mix was calculated from the reagents for the corresponding number of samples of each marker according to the following scheme:

Table 3: Composition of the reaction mixture of the qPCR. The kit used was for cDNA synthesis (AffinityScript qPCR cDNA Synthesis Kit). Experiments were carried out strictly in accordance with the instructions in the kit. Each sample was added to the working solution as follows. cDNA=complementary deoxyribonucleic acid, ROX=carboxy-X-rhodamine, DEPC water = diethyl pyrocarbonate water, µl=microliter.

Component	**Volume (µl)**
cDNA	2
2x SYBR® Green QPCR Master Mix	10
Primer (1x)	2
ROX (30 nmol)	0.3
DEPC water	5.7
Total volume	**20**

The primers used were commercially available from *Biomer.net*, and suitable for use with SYBR Green-based qPCRs. Before use, they were briefly centrifuged according to the manufacturer's instructions and then each primer brought into solution with 1.1 mL TRIS - EDTA buffer solution (TE buffer, pH 8.0) by vortexing.

For relative quantification of the expression of the target genes, the Glyceraldehyde-3-phosphate dehydrogenase (GAPDH) gene was used as a housekeeping gene.

Table 4: Sequences of the forward and reverse primers of the housekeeping gene Glyceraldehyde-3-phosphate dehydrogenase (GAPDH) gene used in qPCR. bp=base pair.

Housekeeping Gene	Primer	Products Length(bp)	T_m (°C)
GAPDH	Forward: GTATGATTCCACCCACGGCA Reverse: CACCCCATTTGATGTTGGCG	243	64 66.6

Table 5: Sequence of target genes. TLR4 = Toll-like receptor 4, NF-κB = nuclear factor kappa B, RANK = receptor-activator of nuclear factor kappa beta, RANKL= receptor-activator of nuclear factor kappa beta ligand, OCN = osteocalcin, OPG = osteoprotegerin, OPN = osteopontin, ALP = alkaline

phosphatase, TGF-β = transforming growth factor-β, IL-2 = interleukin 2, IL-6 = interleukin 6, IL-10 = interleukin 10, T_m = temperature, bp=base pair, °C = degree Celsius, F = forward, R = reverse.

Gene	Primer sequence (5'to3')	Product size(bp)	T_m (°C)
TLR4	F CAGATAAGCGAGGCCGTCATT	113	63,7
	R TTGCAGCCCACAAAAAGCA		63.8
NF-κB	F ACATGGACTTCTCAGCCCTTCTGA	168	65.7
	R CCGAAGACATCACCCAAAGATGCT		67.6
RANK	F GCTGACTCTGGAAGAGAAGGTGTT	192	62.5
	R GCCCTGTCCACATATTCGTCTTCTGT		67.5
RANKL	F GACTTTCAGCAACGGGAAAC	117	59.7
	R AGCTGAAGATACTTCGCATCG		59.6
OCN	F ACGAGCTGGCTGATCACATC	71	61.4
	R CTGCGAGGTCTAGGCTATGC		60.1
OPG	F AAGTCCCGACAGAAGACATCGAGGA	150	68.4
	R GGTACGTCTTGAGATGCTTCAGGGC		68.2
OPN	F GAGCAAACAGACGATGTGGA	150	59.8
	R GAAATCGGTGACCAGCTCAT		60.1
ALP	F AAGAGCATGTGCGGGAAAGT	660	62.1
	R GGAATTCCCAGACAGCACAAA		62.3
TGF-β	F AGGGCTACCATGCCAATTTCT	1021	62
	R CGGGTTGTGCTGGTTGTACA		62.9
IL-2	F CATGCACTAACCCTTGCACTC	80	60.7
	R GGCTCCAGTTGTTTCTTTGTGTT		61.8
IL-6	F GACAAAGCCACCACCCCTAA	69	62.2
	R CTCGTTCTGTGACTGCAGCTTATC		62.7
IL-10	F CCTGACTGCCTCCCACTTTC	94	62.1
	R GGGCTCCCTAGTTTCTCTTCC		60.6

To obtain the final ROX concentration (30 nmol), the stock concentration was diluted 1:500 with diethyl pyrocarbonate (DEPC)-treated water. To identify possible false positive results, 30 ng of genomic porcine DNA was amplified per target gene to be tested. As negative controls, which should represent a situation of absence of mRNA of the target genes, for example to indicate DNA contamination, the templates were replaced by the same volume of RNase-free water in the qPCR reaction mixture (no template control = NTC) or only RNase-free water was pipetted. In addition to the negative controls, templates from porcine liver were used as "positive controls". Each

sample and all controls were determined in duplicates. After pipetting the 96-well plate, it was briefly centrifuged at 3,000g to prevent possible liquid residues on the walls of the wells.

The settings for the various cycles of the qPCR were made using the MxPro program. This was linked to the thermal cycler as well.

Table 6: Cyclic sequence and temperature profiles of RT-qPCR. Total number of cycles is 40. °C= degree Celsius.

Cycle	Time	T_m (°C)
Initial denaturation	3 min	95
Denaturation	20 s	95
Annealing and elongation	20 s	60

2.7.8 Enzyme-Linked immunosorbent Assay (ELISA)

2.7.8.1 Liver Homogenization

The liver tissue had to be homogenized prior to the ELISA. The tissue was cooled all the way through the homogenization period.

The tissue fragments to be homogenized were transferred into 2.0 ml size Eppendorf reaction tubes, and followed by the addition of well diluted (1:20) protease inhibitor cocktail buffer (Sigma) . In order to homogenize thoroughly, the chopped sample (20 mg) was transferred to a tube and homogenized with the oscillator. After mixing all the tissue fragments into a homogeneous solution, the sample was homogenized with ultrasound (BANDELIN) for 3 times at 40-43 kHz for 5 s each time. All the samples were put in a benchtop centrifuge (Thermo Scientific) and centrifuged at 16,000 g for 15 minutes. The supernatant was removed and stored in a 1.5ml Eppendorf reaction tube in a -80 °C freezer.

2.7.8.2 Sandwich ELISA

We took a sandwich ELISA method, and strictly followed the steps listed in the experimental instructions in the kit for analyzing the OPG levels in liver and serum (72 h after the onset of trauma). All samples were diluted 1:2 before measurement.

Table 7: Kit Components (LSBio). ml=milliliter, µl=microliter.

Component	**Quantity**
Coated 96-well Strip Plate	1
Standard (Lyophilized)	2 vials
Sample Diluent	1 vial x 20 ml
Biotinylated Detection Antibody (100x)	1 vial x 120 µl
Biotinylated Detection Antibody Diluent	1 vial x 14 ml
HRP Conjugate (100x)	1 vial x 120 µl
HRP Conjugate Diluent	1 vial x 14 ml
Wash Buffer (25x)	1 vial x 30 ml
TMB Substrate	1 vial x 10 ml
Stop Solution	1 vial x 10 ml
Adhesive Plate Sealers	4
Instruction Manual	1

We brought all reagents and samples to room temperature without additional heating and mixing thoroughly by gently swirling before pipetting. All procedures were carried out in strict accordance to the operating instructions and under the guidance of an experienced technician. The following represents a diagram of the ELISA workflow.

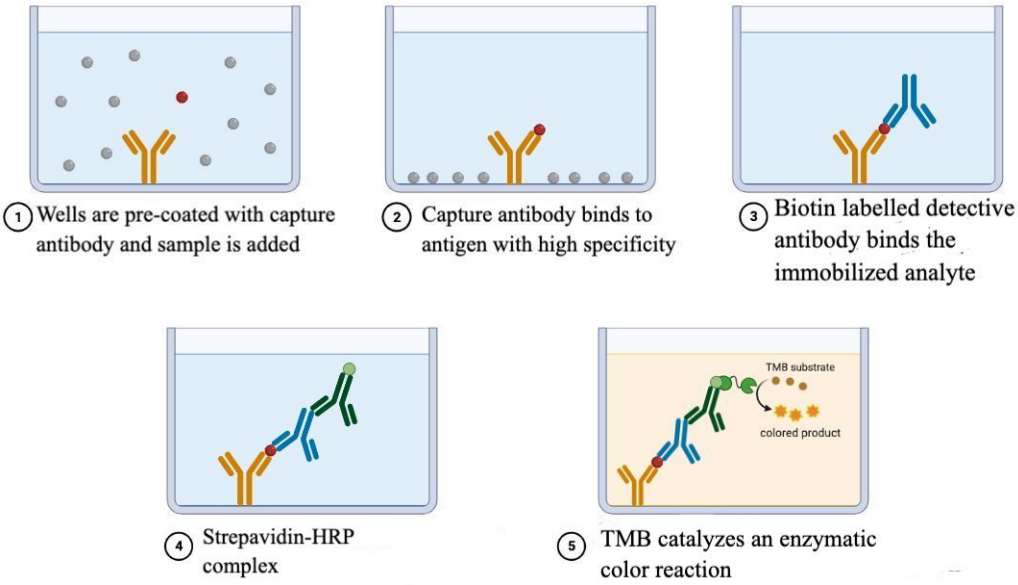

Figure 8: Schematic diagram of ELISA (Sandwich): This ELISA assay is based on the sandwich ELISA principle. Each well of the microtiter plate in this kit was pre-coated with a capture antibody specific to the target. After the standard or sample was added to the wells, the target antigen bound to the capture antibody and the unbound antigen was washed away. A biotin-conjugated detection antibody was then added to bind to the captured antigen. The unbound biotin antibody was washed away. Next Avidin-Horseradish Peroxidase (HRP) conjugate was then added which binds to the biotin and the unbound HRP conjugate was washed off. Finally, the TMB substrate was added to develop the color in reaction with the HRP enzyme. Sulphuric acid termination solution was added to terminate the color development reaction and the optical density was measured at 450 nm. The images were made by myself with the BioRender drawing tool.

2.7.8.3 Competitive ELISA

We took a competitive ELISA method, and strictly followed the steps listed in the experimental instructions in the kit for analyzing the RANK and RANKL levels in liver and serum (72 h after the onset of trauma). All samples were diluted 1:2 before measurement.

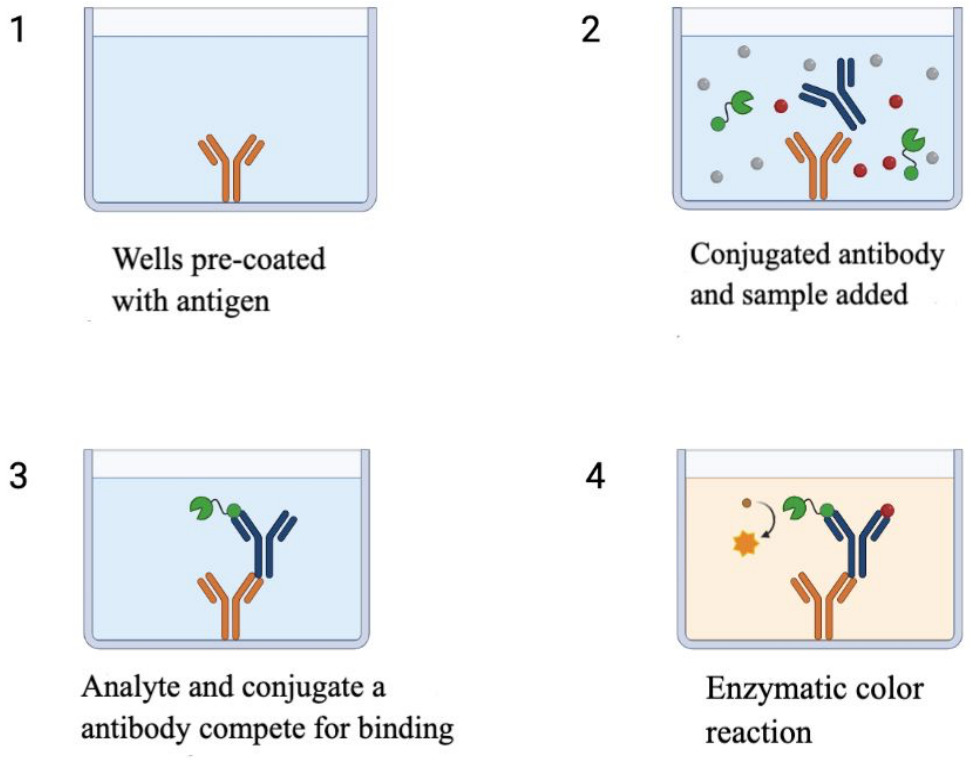

Figure 9: Schematic diagram of a competitive ELISA. Competitive ELISA, also known as blocking ELISA, is based on the principle that the antigen in the sample and a specific amount of enzyme-labeled antigen compete for binding to the solid-phase antibody. The amount of antigen in the sample had an inverse ratio to the bound to the solid of the enzyme-labeled antigen, i.e., the final color rendering result is negatively correlated with the interference level of the antigen or antibody to be detected. The images were made by myself with the BioRender drawing tool.

RANK, RANKL and OPG concentrations in liver tissue of pigs and 72 hours after the onset of trauma were measured using a commercially available enzyme-linked immunosorbent assay (ELISA) kit strictly in accordance to the manufacturer's protocol. As a first step, a specific antibody was applied to a plate to capture the analyte. Standard and samples were being incubated with the solid phase antibody, which captured the analyte. In order to detect the analyte, a detection antibody conjugated with biotin was added following the washing of unbound analyte. All unbound detection antibodies should be removed after a wash. In addition, the detection reagent (streptavidin-HRP) was added. The color was developed in proportion to the number of analytes bound on the plate after incubation with a

substrate solution (TMB/hydrogen peroxide). Color development was stopped by a sulphuric acid termination solution and OD value was measured at 450 nm.

2.7.9. BCA Protein analysis

Based on bicinchoninic acid (BCA), PierceTM bicinchoninic acid (BCA) Protein Assay kit quantifies total protein using a detergent-compatible formulation. A series of dilutions of bovine serum albumin (BSA) were prepared for the standard curve. 10 µl of diluted samples were added to 96-well plates. To make the working BCA reagent, 50 parts of BCA Reagent A were mixed with 1 part of BCA Reagent and 200 µl were added to each well. A optical density measurement was conducted at 562 nm following 30 min of incubation at 37 ℃.

2.7.10 Immunohistochemical staining of Myeloperoxidase (MPO)

Formalin-fixed paraffin-embedded liver slides (4 µm thickness) were deparaffinized and rehydrated in a descending alcohol series. The antigen retrieval was performed in a microwave (700 W) using citrate buffer (pH 6.0). The slides were blocked with 10% normal goat serum for 1 h at RT. Afterwards the slides were incubated with a primary antibody (rabbit anti-pig MPO polyclonal antibody, Abcam, Cambridge) at a concentration of 1.4 µg/ml at 4 °C overnight. The MPO detection was based on alkaline phosphatase method using DAKO kit. Seven pictures at 20x were taken from each slide and analyzed using ImageJ automated cell-counting.

2.7.11 Statistical analysis

To check the normality of the obtained data sets, the Shapiro–Wilk test and the Kolmogorov-Smirnov test were performed on each set of data. Data satisfying normal distribution were expressed as mean ± standard error of the mean (SEM). A t-test was

performed between two groups. A chi-square test or ANOVA was performed for comparisons between multiple groups. Data that did not satisfy a normal distribution were subjected to the rank sum test. A $p<0.05$ was considered statistically significant.

3. Results

3.1 Liver injury score

The analysis of the HE-stained slides of liver tissue taken 72 hours after the traumatic impact revealed a significant increase of the damage score in both PT + HS groups versus the sham group (Fig.10). The liver injury score of the Nail+ Therapy group was significantly lower than in the Nail group alone without additional immune therapy (Fig. 10a).

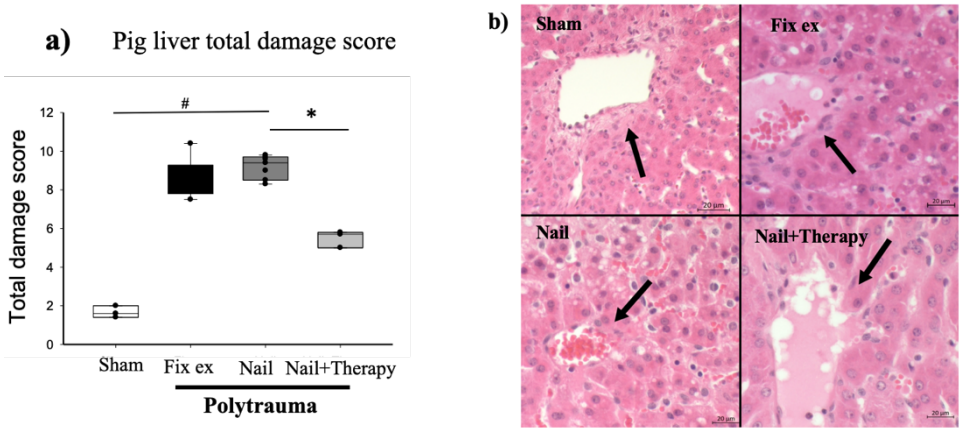

Figure 10: Liver injury score (a) Liver samples were obtained from pigs in each group 72 h post polytrauma and paraffin sections were made. H&E-staining evaluation and observed under a 400x microscope for further scoring. Statistical plot of the overall mean score for liver damage in each group (a). Histological changes in the liver of each group of pigs as observed microscopically after HE staining (b). The black arrow indicates the structure of the liver lobules. *p<0.05 vs. sham, #p<0.05 vs. Therapy. Nail=Internal fixation with intramedullary nail, Fix ex = External fixation. Nail+Therapy = intramedullary nail with combined complement 5/cluster of differentiation 14 (C5/CD14) inhibitor treatment. Sham: n = 6, Nail: n = 7, Fix ex: n = 8, Nail+Therapy: n = 4.

HE staining showed that 72 hours after the polytrauma, the morphology of the liver tissue exhibited a large number of vacuoles (Fig. 12) compared to the normal control group, with varying degrees of disorganization and congestion of the hepatic lobular structure (Fig. 11), and necrosis of some hepatocytes (Fig. 13) was visible. The inflammatory reaction of the liver tissue was obvious and neutrophil infiltration was seen (Fig. 14). At the same time, the degree of necrosis, hepatic lobular stasis and

inflammation were significantly reduced in the polytrauma group treated with C5/CD14 immunosuppression. The total score for each group was 1.67±0.31 for the Sham group, 8.65±1.01 for the Fix ex group, 9.19±0.60 for the Nail group and 5.50±0.44 for the Nail+Therapy group.

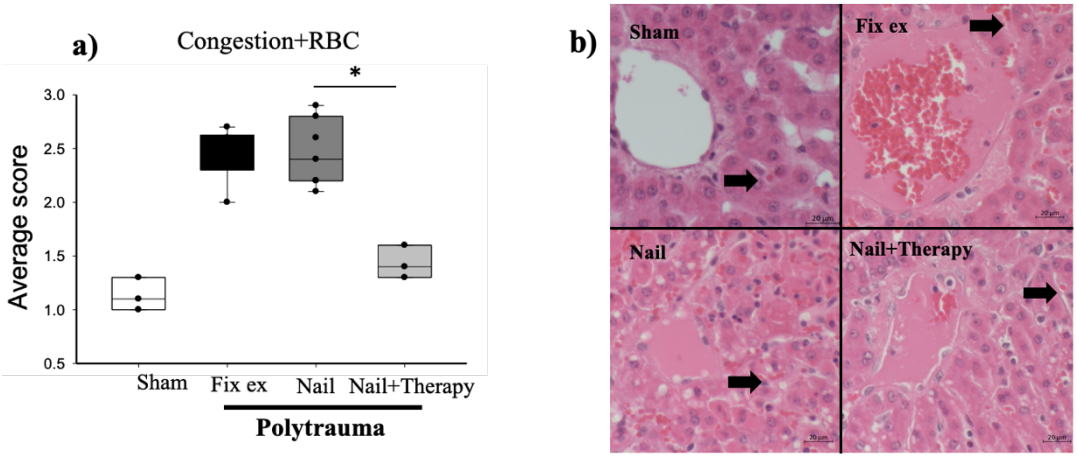

Figure 11: Congestion. Liver samples were obtained from pigs in each group after 72 h of euthanasia and paraffin sections were made. They were stained with H&E and observed under a 400x microscope for further scoring. Rank sum test statistical methods were used to compare the data between Nail and Nail+Therapy. Statistical plot of the overall mean score for congestion (RBC) in each group (a). The black arrow indicates the presence of congestion or RBC in the structures of the hepatic lobules (b). *p<0.05 vs. Therapy, # p<0.05 vs. sham. Nail = Internal fixation with intramedullary nail, Fix ex = External fixation. Nail+Therapy = intramedullary nail with combined complement 5/cluster of differentiation 14 (C5/CD14) inhibitor treatment. Sham: n = 6, Nail: n = 7, Fix ex: n = 8, Nail+Therapy: n = 4.

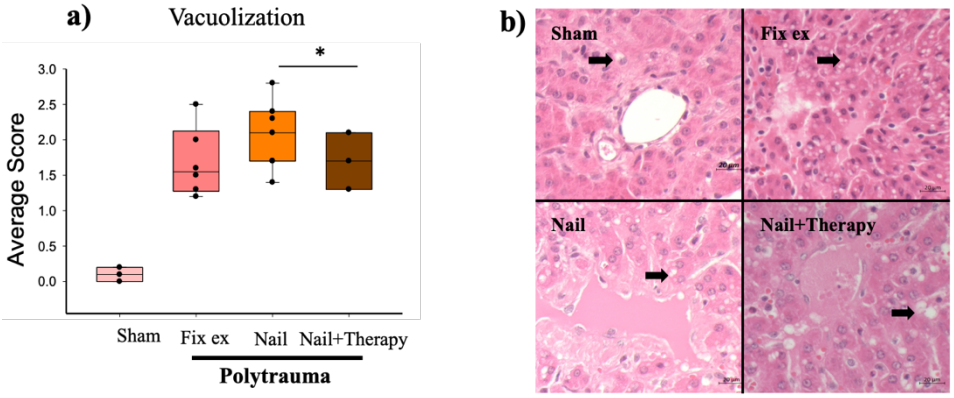

Figure 12: Vacuolization. Liver samples were obtained from pigs in each group 72h of the polytrauma and paraffin sections were made. They were stained with H&E and observed under a 400x microscope for further

scoring. Rank sum test statistical methods were used to compare the data between Nail and Nail+Therapy. Statistical plot of the overall mean score for vacuolization in each group (a). The black arrow indicates the presence of vacuolization in the structures of the hepatic lobules (b). *p<0.05 vs. Nail+Therapy, # p<0.05 vs. sham. Nail = Internal fixation with intramedullary nail, Fix ex = External fixation. Nail+Therapy = intramedullary nail with combined complement 5/cluster of differentiation 14 (C5/CD14) inhibitor treatment. Sham: n = 6, Nail: n = 7, Fix ex: n = 8, Nail+Therapy: n = 4.

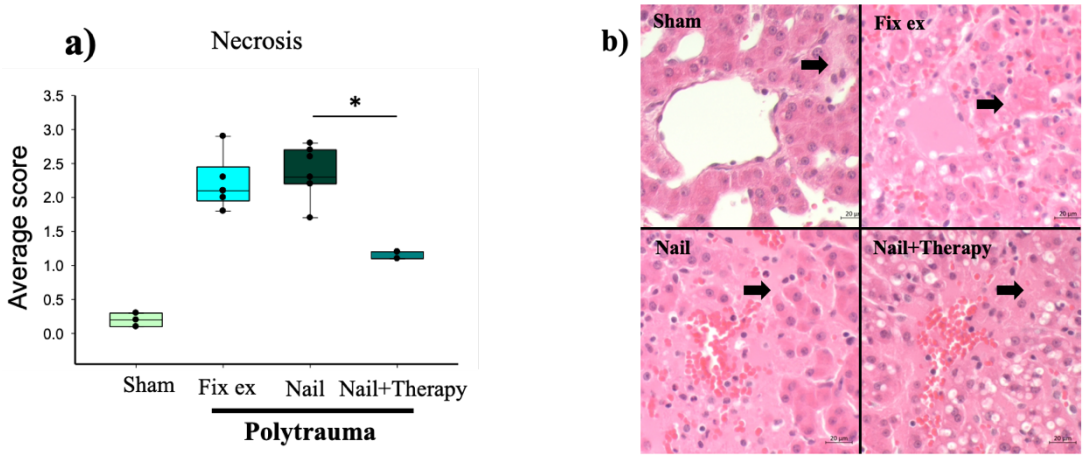

Figure 13: Necrosis. Liver samples were obtained from pigs in each group 72 h after polytrauma and paraffin sections were made. H&E-staining, evaluated under a 400x microscope. Rank sum test statistical methods were used to compare the data between Nail and Nail+Therapy. Necrotic liver tissue is light in color and poorly bordered by the surrounding tissue. Statistical plot of the overall mean score for necrosis in each group (a). The black arrow indicates the presence of necrosis in the structures of the hepatic lobules (b). *p<0.05 vs. Therapy, # p<0.05 vs. sham. Nail = Internal fixation with intramedullary nail, Fix ex = External fixation. Nail+Therapy = intramedullary nail with combined complement 5/cluster of differentiation 14 (C5/CD14) inhibitor treatment. Sham: n = 6, Nail: n = 7, Fix ex: n = 8, Nail+Therapy: n = 4.

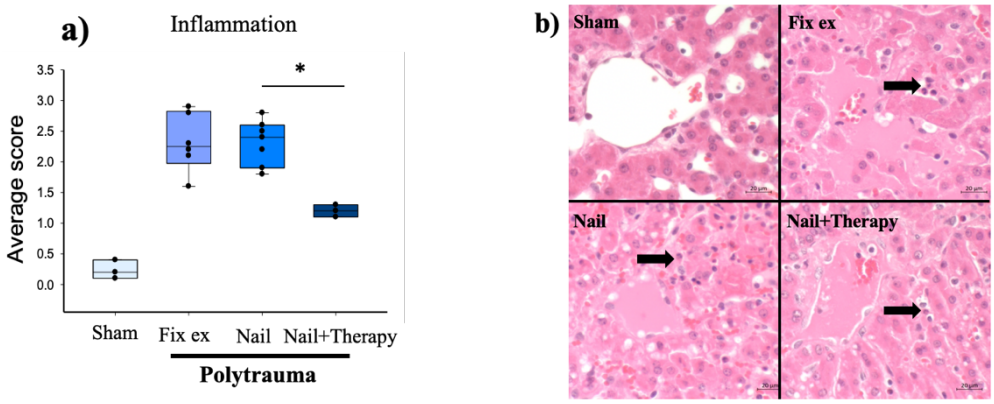

Figure 14: Inflammation (number of neutrophils). Liver samples were obtained from pigs in each group 72 h after polytrauma and paraffin sections were made. They were stained with H&E and observed under a 400x microscope for further scoring. Rank sum test statistical methods were used to compare the data between Nail and Nail+Therapy. Necrotic liver tissue is light in color and poorly bordered by the surrounding tissue. Statistical plot of the overall mean score for the number of PMN in each group (a). Histological changes in the liver of each group of pigs as observed microscopically after HE staining (b). The black arrow indicates the presence of inflammation or PMN in the structures of the hepatic lobules. *p<0.05 vs. Therapy, # p<0.05 vs. sham. Nail = Internal fixation with intramedullary nail, Fix ex = External fixation. Nail+Therapy = intramedullary nail with combined complement 5/cluster of differentiation 14 (C5/CD14). Sham: n = 6, Nail: n = 7, Fix ex: n = 8, Nail+Therapy: n = 4. Data as mean ± standard deviation.

3.2 ALP, ALT, AST and protein concentrations in serum

Abnormal levels of ALP in the blood may indicate problems related to the liver, gallbladder or bones. The levels of ALP (Table 8) in the sham group showed a decreasing trend over time. ALP levels in the polytrauma and treatment groups showed a trend of increasing and then decreasing, indicating a degree of remission of inflammation levels in vivo at a later stage. Values for each group re expressed as the mean ± SEM of each group and plotted as a graph or a table.

ALT and AST are widely present in hepatocytes and are two important indicators of hepatocyte damage and the extent of the corresponding damage. When the liver was damaged, enzymes such as AST and ALT were released from the liver cells into the blood. The total serum AST (Table 9) level in normal control pigs was 29.00±19.76 U/L. Traumatic blood loss caused liver damage in pigs. At the beginning of the trauma, there was no significant increase in serum AST levels in pigs ($p>0.05$). At 1.5 h after trauma, the AST level in the Nail group increased significantly compared to the normal control group (55.57±25.09 U/L vs. 26.67±14.11 U/L), suggesting that the liver of pigs had been significantly damaged 1.5 h after trauma. As time passed, we could find that the peak values were reached at 48 h after the trauma (33.00±19.60, 81.38±59.21, 47.86±16.65, 46.00±17.09, table 9) and then decreased again.

The ALT (Table 10) levels in the serum of the pigs in each group fluctuated considerably during the 72-h following the onset of trauma. ALT in the Nail group showed a consistent upward trend, but the treatment group using the combined C5/CD14 inhibitor represented lower ALT levels than the Nail group ($p<0.05$). The serum ALT level in the normal control group was 41.83±10.98 at 0 h. At the beginning of the trauma, there was no significant change in the Sham, Nail and Fix ex groups, except for the Nail+Therapy group where the ALT level was higher than the sham group ($p<0.05$). Serum ALT levels in all four groups showed an overall stable trend over time, but ALT levels in the Nail group and the Nail+Therapy group increased 72 h after the trauma and were higher in the nail group than in the Nail+Therapy group ($p<0.05$).

Decreasing trend in the amount of the serum protein (Table 11) over time was found. The amount of protein in the serum at each time point was higher in the trauma sham group than in the Nail+Therapy group ($p<0.05$). The amount of protein in the serum in the nail group was higher than in the Nail+Therapy group at 0 h, 2.5 h, 24 h and 72 h after the onset of trauma ($p<0.05$).

Table 8 ALP levels in serum at different time points (U/L). Significantly higher protein level in the Sham group compared to the trauma group, *$p<0.05$. Significantly higher protein level in the Nail group compared to the Nail+Therapy group, # $p<0.05$. Nail = Internal fixation with intramedullary nail, Fix ex = External fixation. Nail+Therapy = intramedullary nail with combined complement 5/cluster of differentiation 14 (C5/CD14). Sham: n = 6, Nail: n = 7, Fix ex: n = 8, Nail+Therapy: n = 4. Data as mean ± standard deviation.

Time	Sham	Nail	Fix ex	Nail+Therapy
0h	111.5±50.49	94.75±20.01	113.63±52.29	144.50±32.58
1.5h	103.33±43.10	94.88±17.75#	125.50±35.10	138.25±23.92
2.5h	103.67±43.03	91.13±19.37#	118.88±33.03	132.50±31.14
24h	100.20±38.54	118.75±29.63#	151.75±45.37*	187.25±52.65*
48h	76.67±31.61	101.88±38.82#	136.50±41.01*	153.25±23.06*
72h	79.50±30.59	80.50±13.50	101.43±27.61	97.50±65.52

Table 9 AST levels in serum at different time points (U/L). Significantly higher protein level in the Sham group compared to the trauma group, *p<0.05. Significantly higher protein level in the Nail group compared to the Nail+Therapy group, #p<0.05. Nail = Internal fixation with intramedullary nail, Fix ex = External fixation. Nail+Therapy = intramedullary nail with combined complement 5/cluster of differentiation 14 (C5/CD14). Sham: n = 6, Nail: n = 7, Fix ex: n = 8, Nail+Therapy: n = 4. Data as mean ± standard deviation.

Time	Sham	Nail	Fix ex	Nail+Therapy
0h	29.00±19.76	42.75±36.16	24.37±8.96	23.75±5.43
1.5h	26.67±14.11	55.57±25.09*	41.50±16.94	36.75±13.30
2.5h	27.00±13.84	71.63±55.88*	40.88±13.50	36.00±9.83
24h	32.67±25.63	76.38±44.42*	47.00±12.12	43.75±13.05
48h	33.00±19.60	81.38±59.21*	47.86±16.65	46.00±17.09
72h	25.33±8.64	56.57±41.68*#	33.14±18.01	26.33±6.11

Table 10 ALT levels in serum at different time points post trauma (U/L). Significantly higher ALT in the trauma group compared to the Sham group, *p<0.05. Nail = Internal fixation with intramedullary nail, Fix ex = External fixation. Nail+Therapy = intramedullary nail with combined complement 5/cluster of differentiation 14 (C5/CD14). Sham: n = 6, Nail: n = 7, Fix ex: n = 8, Nail+Therapy: n = 4. Data as mean ± standard deviation.

Time	Sham	Nail	Fix ex	Nail+Therapy
0h	41.83±10.98	45.43±10.13	43.63±10.53	60.25±16.03*
1.5h	41.33±12.37	44.63±8.68	45.25±9.39	58.00±16.41*
2.5h	41.33±11.71	49.50±9.94	44.88±10.95	58.50±15.02*
24h	35.33±7.94	47.50±16.48	44.13±6.40	52.50±13.87*
48h	33.67±12.63	52.25±17.27	43.25±6.99	52.25±17.27*
72h	33.00±9.68	65.33±7.57*	41.14±4.74	57.00±13.53*

Table 11 Protein concentration in serum at different time points post trauma (g/dL). Significantly higher protein level in the Sham group compared to the trauma group, *p<0.05. Significantly higher protein level in the Nail group compared to Nail+Therapy group, #p<0.05. Nail = Internal fixation with intramedullary nail, Fix ex = External fixation. Nail+Therapy = intramedullary nail with combined complement 5/cluster of differentiation 14 (C5/CD14). Sham: n = 6, Nail: n = 7, Fix ex: n = 8, Nail+Therapy: n = 4. Data as mean ± standard deviation.

Time	Sham	Nail	Fix ex	Nail+Therapy
0h	4.73±0.30	4.57±0.41#	4.43±0.22	4.15±0.19*
1.5h	4.50±0.28	4.27±0.34	4.25±0.28	4.03±0.29*
2.5h	4.47±0.25	4.11±0.33#	4.09±0.25*	3.83±0.17*
24h	3.90±0.24	3.60±0.36#	3.68±0.17	3.18±0.29*
48h	3.68±0.26	3.41±0.34	3.54±0.19	3.20±0.19*
72h	3.92±0.50	3.60±0.19#	3.60±0.27	2.65±1.11*

3.3 Myeloperoxidase (MPO) activity

Seven observation fields were taken for each tissue sample after immunohistochemical staining, and the number of positive signal cells was recorded using ImageJ. The average number of MPO positive cells (Fig.17) in each group was finally calculated. Few MPO positive signals were seen in the liver tissues of the control pigs, whereas MPO positive signals were increased in the liver tissues in polytraumatized pigs treated by either the internal or external fixation. Statistical analysis revealed that the number of MPO positive cells in the internal fixation group was 2.5±2.4 times higher than that in the control group ($p=0.038$), while there are no differences between the remaining groups ($p>0.05$). Of note, a significant decrease in MPO staining was found in livers from polytraumatized pigs treated with a Nail and combined C5/CD14 blockade versus the Nail only group.

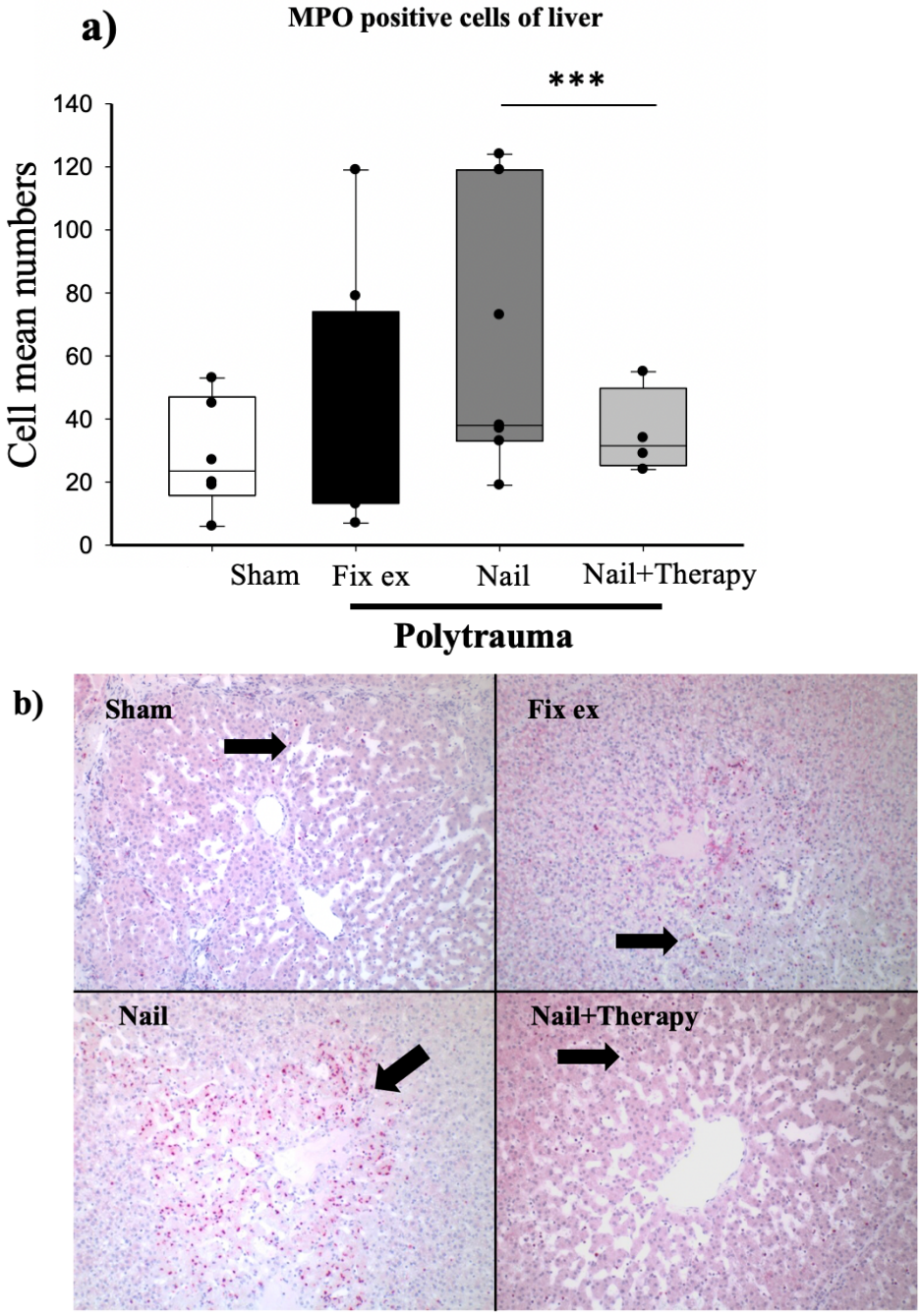

Figure 15: Results of myeloperoxidase (MPO) staining of liver samples from different groups of pigs. Liver samples were obtained from pigs in each group after 72 h after polytrauma or sham procedure and paraffin sections were made. They were stained with primary antibody rabbit anti-pig MPO polyclonal antibody and observed under a 100x microscope for further scoring. ANOVA method was used to compare the data between the groups. Statistical plot of the overall mean score for cell number in each group (a). Histological changes in the liver of each group of pigs as observed microscopically after MPO staining (b). The black arrow indicates the MPO positive cells in the structures of the hepatic lobules. *$p<0.05$ vs. Therapy. Nail = Internal fixation with intramedullary nail, Fix ex = External fixation. Nail+Therapy = intramedullary nail with combined complement 5/cluster of differentiation 14 (C5/CD14). Sham: n = 6, Nail: n = 7, Fix ex: n = 8, Nail+Therapy: n = 4. Data as mean ± standard deviation.

3.4 Vital signs temperature and central venous pressure.

The overall trend of the tail temperature (Fig.16) was similar in all four groups. The experimental animals in the Nail and Fix ex groups experienced a slight decrease in body temperature for 1-1.5 h after the onset of trauma, followed by a progressive increase and finally a peak within 7-9 h of trauma onset, followed by a plateau phase. Notably, the pigs in the C5/CD14 immunosuppressed group and the sham group did not experience this initial alteration of the body temperature, but also reached a peak within 7-9 h of trauma occurrence.

Concerning the central venous pressure (CVP), during the first 9 hours, all four groups of experimental animals showed a fluctuating course (Fig.17). Afterwards, the CVP was more stable in all groups.

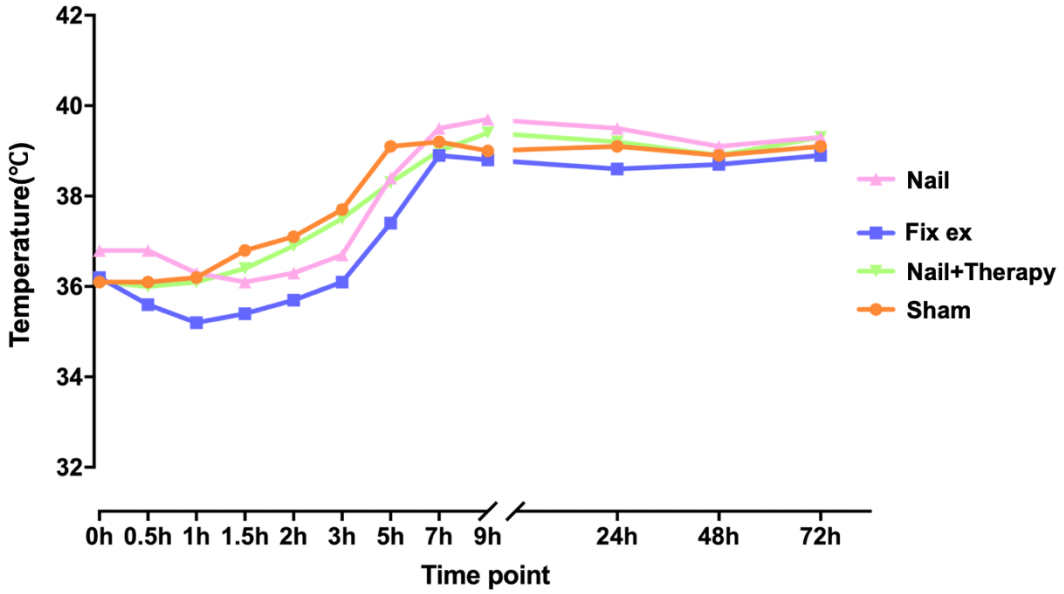

Figure 16: Time course of body temperature. The intra-nasal temperature of individual pigs was measured with a temperature sensor for 72 hours post-trauma, connected to an ECG monitor to obtain temperature results in real time. Presentation of the mean value of the different groups. Data show mean values of n = 4-8 in per time point. Nail = Internal fixation with intramedullary nail, Fix ex = External fixation. Nail+Therapy = intramedullary nail with combined complement 5/cluster of differentiation 14 (C5/CD14). Sham: n = 6, Nail: n = 7, Fix ex: n = 8, Nail+Therapy: n = 4. Data as mean ± standard deviation.

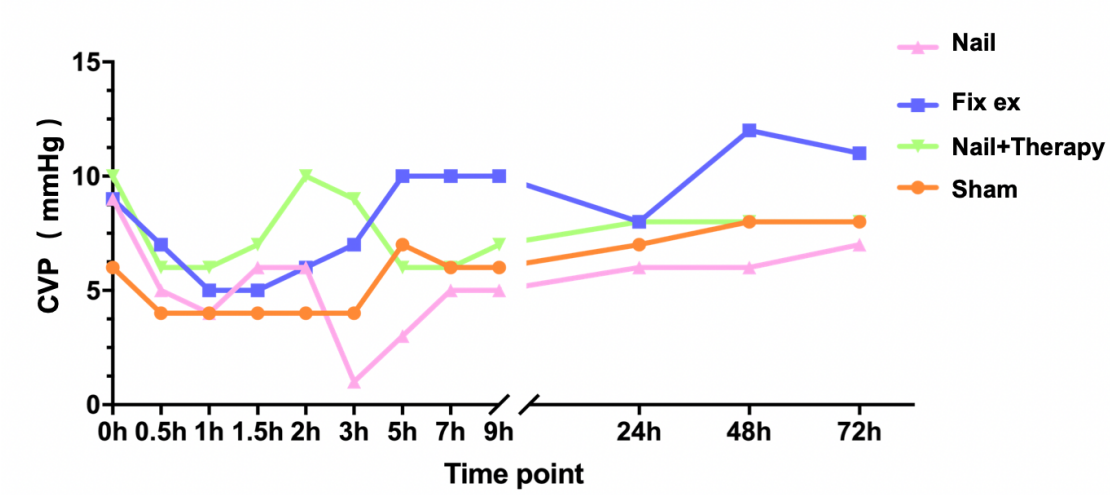

Figure 17: Time course of central venous pressure (CVP). Monitoring of the CVP in real time. Data show mean values of n = 4-8 in per time point. Nail = Internal fixation with intramedullary nail, Fix ex = External fixation. Nail+Therapy = intramedullary nail with combined complement 5/cluster of differentiation 14 (C5/CD14). Sham: n = 6, Nail: n = 7, Fix ex: n = 8, Nail+Therapy: n = 4. Data as mean ± standard deviation.

3.5 Gene expression in the liver tissue.

The gene expression of key bone modifiers, that is RANK, RANKL and OPG was determined in the liver (Fig 18 A, B, C, respectively). For RANK, its levels were significantly higher in the Nail group than in the sham and treatment groups. For RANKL, the levels were significantly higher in the Nail group than in the Nail+Therapy group ($p<0.05$). The gene expression of ALP, OCN and OPN (Fig 18 D,E,F, respectively) was higher in the livers of the nail group than in the Nail+Therapy group ($p<0.05$).

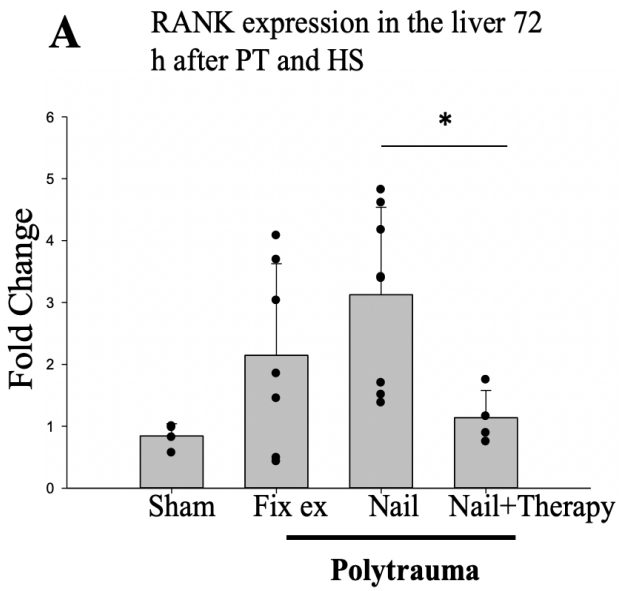

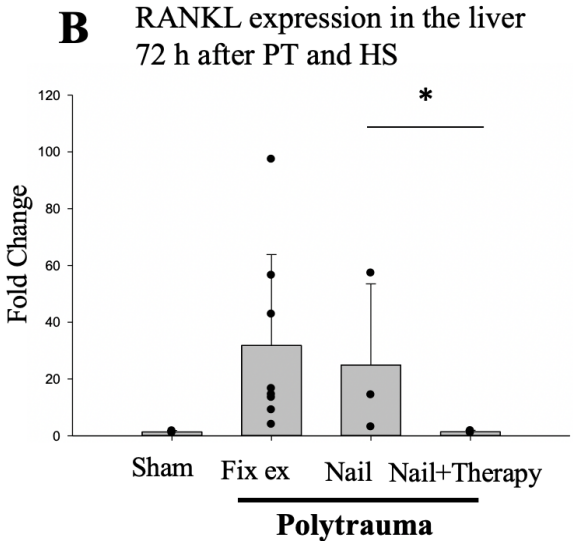

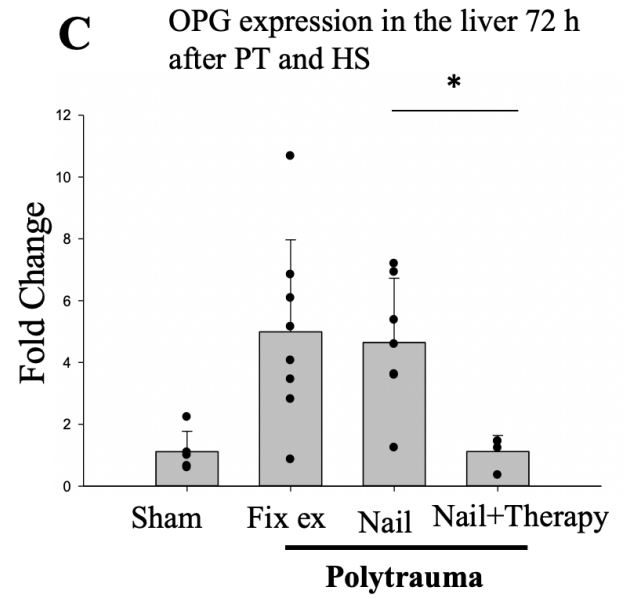
C
OPG expression in the liver 72 h after PT and HS
*
Fold Change
12
10
8
6
4
2
0
Sham
Fix ex
Nail
Nail+Therapy
Polytrauma

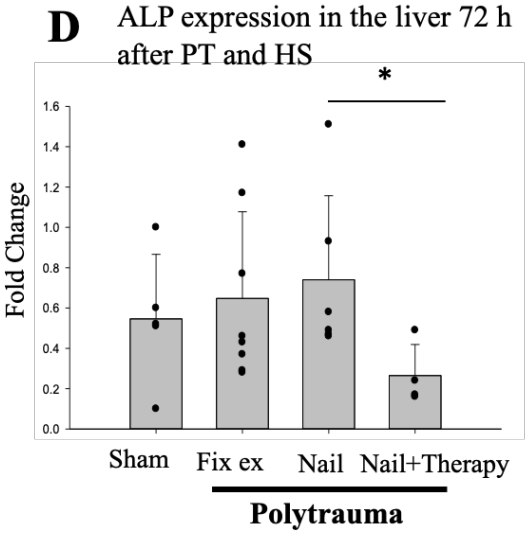
D
ALP expression in the liver 72 h after PT and HS
*
Fold Change
1.6
1.4
1.2
1.0
0.8
0.6
0.4
0.2
0.0
Sham
Fix ex
Nail
Nail+Therapy
Polytrauma

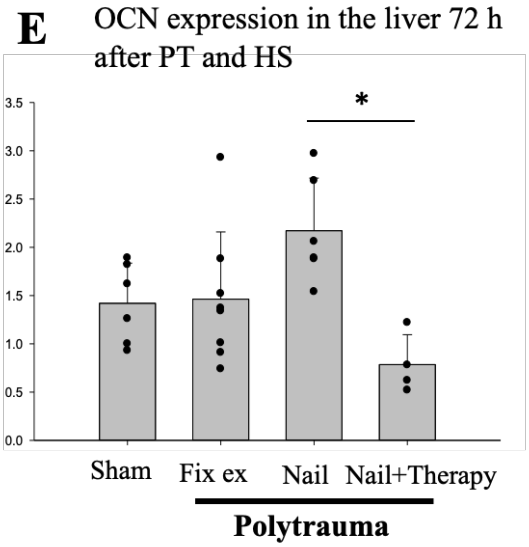
E
OCN expression in the liver 72 h after PT and HS
*
3.5
3.0
2.5
2.0
1.5
1.0
0.5
0.0
Sham
Fix ex
Nail
Nail+Therapy
Polytrauma

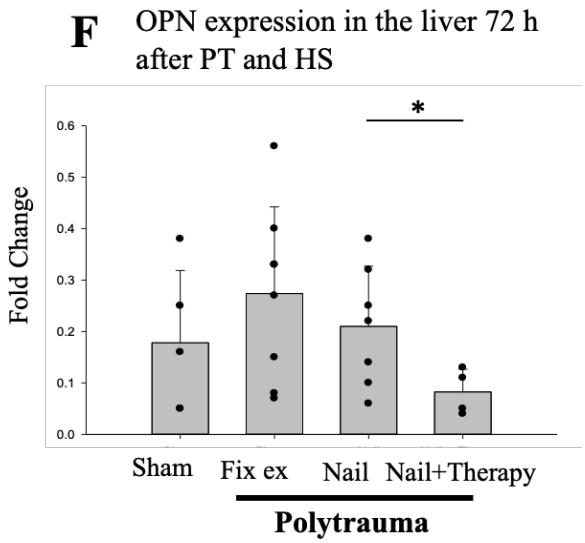

Figure 18: Gene expression of bone-related modifiers in liver samples after polytrauma. A: RANK = receptor activator of nuclear factor-κB. B: RANKL = receptor activator of nuclear factor-κB-ligand. C: OPG = osteoprotegerin. D:ALP = alkaline phosphatase. E: OCN = osteocalcin. F: OPN = osteopontin**.** All samples were homogenized and RNA isolated and subsequently processed for cDNA synthesis and final target gene measurement. The housekeeping gene used was Glyceraldehyde-3-phosphate Dehydrogenase (GADPH) and the ΔΔCt value was calculated from the measurements and the final expression of the target gene in the samples. Data represent means ± SD. Data satisfying a normal distribution were subjected to a ANOVA, otherwise the rank sum test was used. Nail = Internal fixation with intramedullary nail, Fix ex = External fixation. Nail+Therapy = intramedullary nail with combined complement 5/cluster of differentiation 14 (C5/CD14) inhibitor treatment. * $p<0.05$, ** $p<0.01$, ***$p<0.001$. Sham: n = 6, Nail: n = 7, Fix ex: n = 8, Nail+Therapy: n = 4.

For the three factors of IL-2, IL-6 and IL-10 (Fig.19 B, C, A, respectively), gene expression in the liver was higher in the nail group than in the Nail+Therapy group ($p<0.05$). It is worth noting that IL-10 levels were also significantly higher in the Nail group than in the Nail+Therapy group, $p<0.001$.

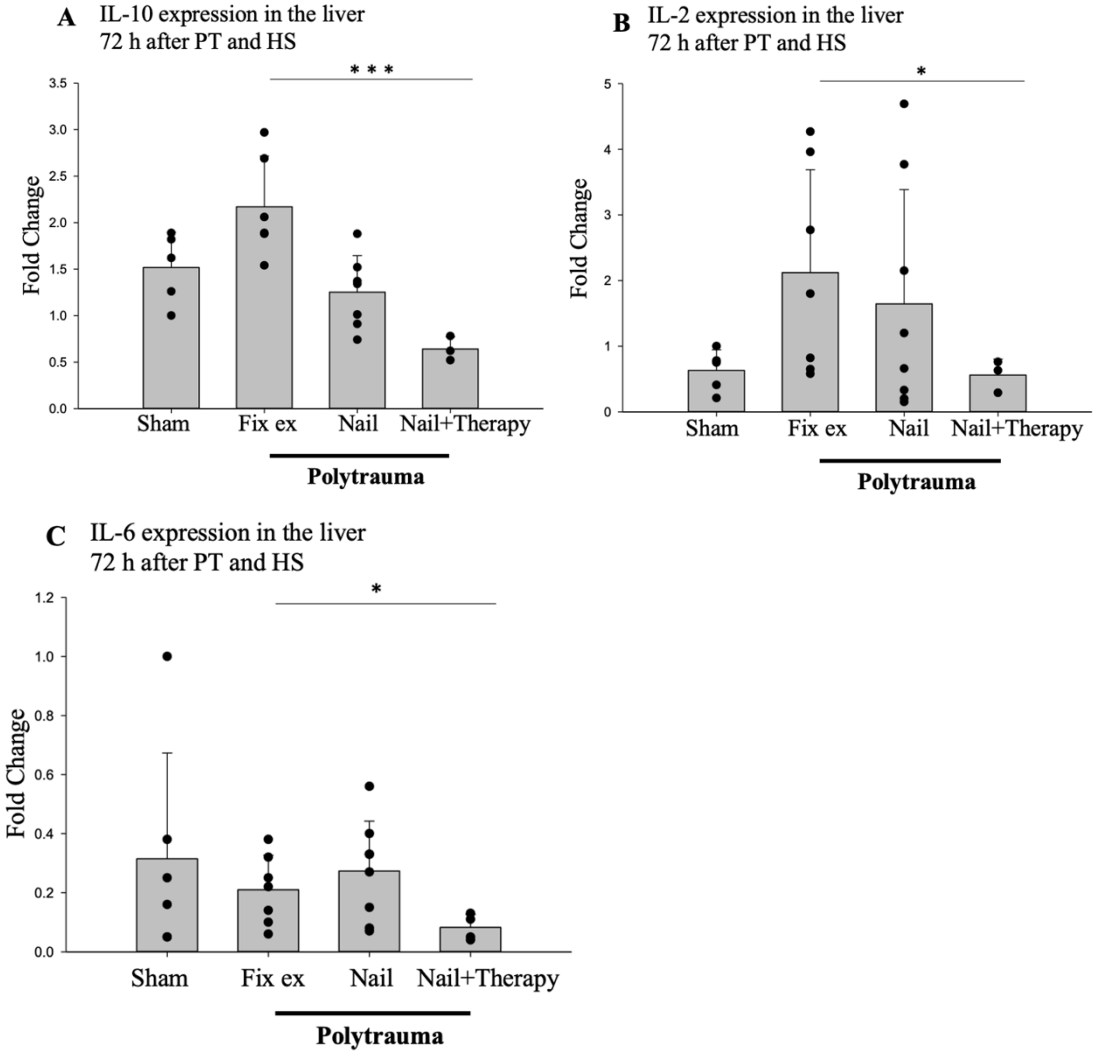

Figure 19: Gene expression of makers of the inflammation in the liver after polytrauma. A: IL-10 = interleukin-10, B: IL-2 = interleukin-2, C: IL-6 = interleukin-6. Results of PCR for three kinds of interleukins in liver samples. All samples were homogenized and RNA isolated and subsequently processed for cDNA synthesis and final target gene measurement. The housekeeping gene used was Glyceraldehyde-3-phosphate Dehydrogenase (GADPH) and the ΔΔCt value was calculated from the measurements and the final expression of the target gene in the samples. Data represent means ± SD. Data satisfying a normal distribution were subjected to a ANOVA, otherwise the rank sum test was used. Nail = Internal fixation with intramedullary nail, Fix ex = External fixation. Nail+Therapy = intramedullary nail with combined complement 5/cluster of differentiation 14 (C5/CD14) inhibitor treatment. * $p<0.05$, ** $p<0.01$, ***$p<0.001$. Sham: n = 6, Nail: n = 7, Fix ex: n = 8, Nail+Therapy: n = 4.

3.6 Protein level of OPG, RANK, RANKL in liver and serum

The protein calculation of OPG (Fig. 20 A) and RANK (Fig. 21 A) in the liver of the nail group were higher than those of the sham group or the therapy group ($p<0.05$). Interestingly, RANKL levels (Fig. 22 A) were higher in liver samples from the Nail+Therapy group than the nail group alone ($p<0.05$). The levels of OPG, RANK and RANKL (Fig. 22 B, 23B and 24B, respectively) in the 72 h serum were all higher in the Nail group than in the Nail+Therapy group ($p<0.05$).

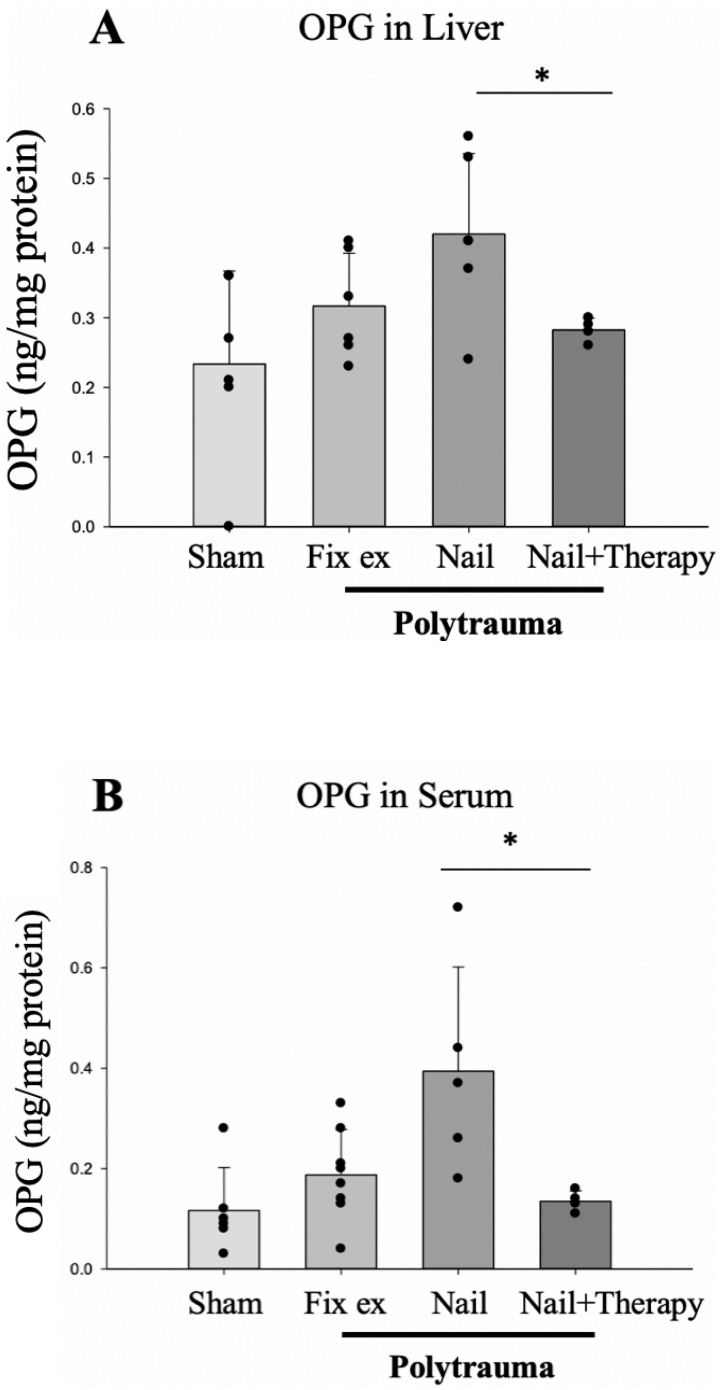

Figure 20: Levels of OPG protein in liver tissue (A) and serum (B). Osteoprotegerin (OPG) levels were measured by enzyme-linked immunosorbent assays (ELISA) in liver tissue homogenates and serum samples after 72h after polytrauma. The Nail group and Nail+Therapy group were analysed by ANOVA and the data were tested by rank sum test if the normality test was not satisfied. Nail = Internal fixation with intramedullary nail, Fix ex = External fixation. Nail+Therapy = intramedullary nail with combined complement 5/cluster of differentiation 14 (C5/CD14) inhibitor treatment. * $p<0.05$, ** $p<0.01$, ***$p<0.001$. Sham: n = 6, Nail: n = 7, Fix ex: n = 8, Nail+Therapy: n = 4.

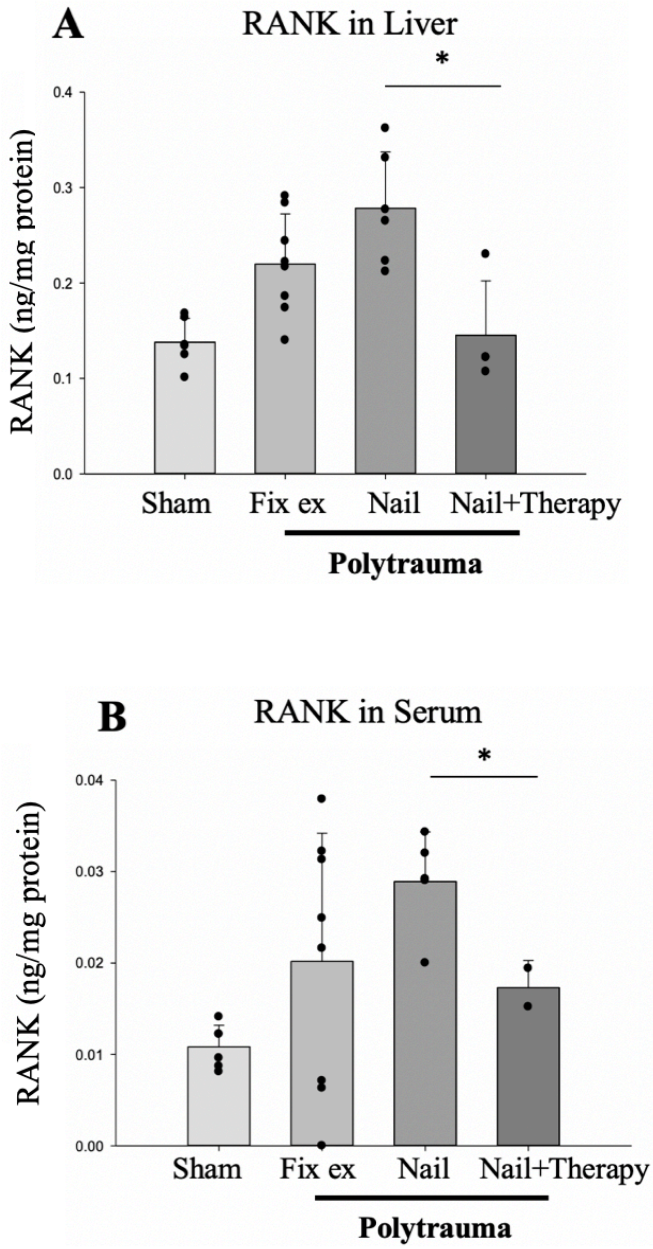

Figure 21: Levels of RANK protein in liver tissue (A) and serum (B). Receptor activator of nuclear factor-κB (RANK) levels were measured by enzyme-linked immunosorbent assays (ELISA) in liver tissue homogenates and serum samples 72 h after polytrauma. The Nail group and Nail+Therapy group were analysed by ANOVA and the data were tested by rank sum test if the normality test was not satisfied. Nail = Internal fixation with intramedullary nail, Fix ex = External fixation. Nail+Therapy = intramedullary nail with combined complement 5/cluster of differentiation 14 (C5/CD14) inhibitor treatment. * $p<0.05$, ** $p<0.01$, ***$p<0.001$. Sham: n = 6, Nail: n = 7, Fix ex: n = 8, Nail+Therapy: n = 4.

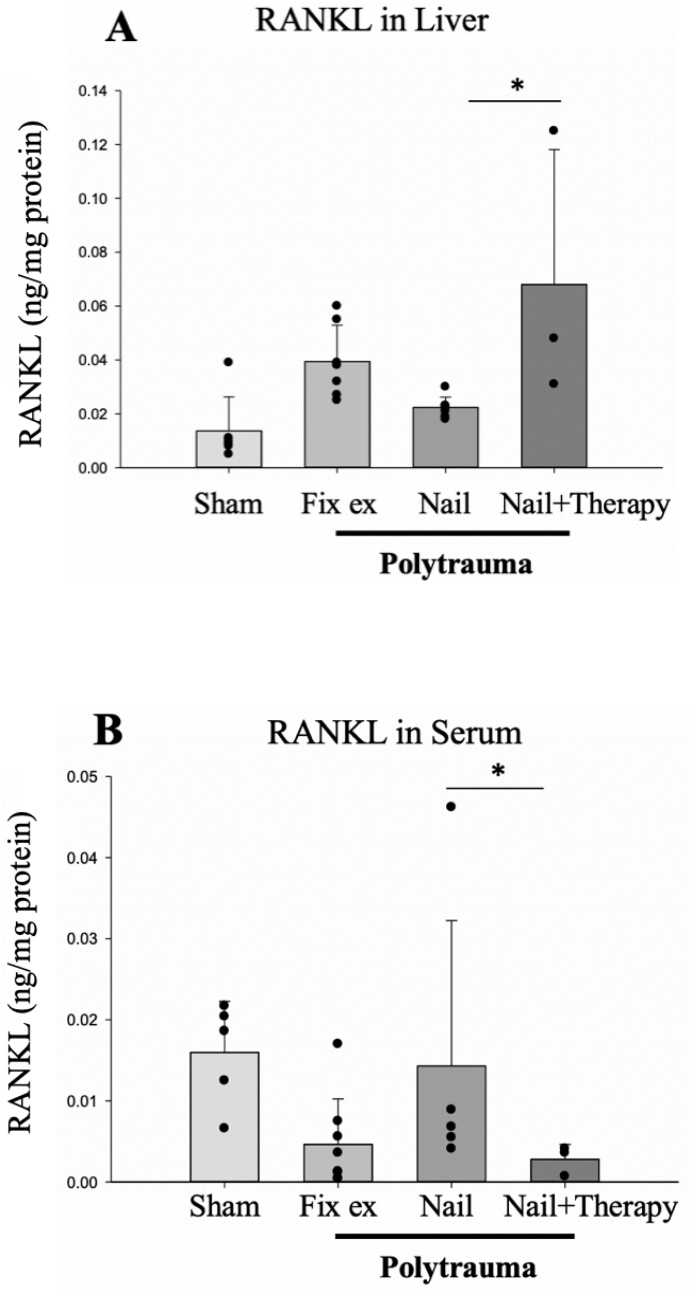

Figure 22: Levels of RANKL protein in liver tissue (A) and serum (B). Receptor activator of nuclear factor-κB-ligand (RANKL) concentrations were measured by enzyme-linked immunosorbent assays (ELISA) in liver tissue homogenates and serum samples 72 h after polytrauma. The Nail group and Therapy group were analysed by ANOVA and the data were tested by rank sum test if the normality test was not satisfied. Nail = Internal fixation with intramedullary nail, Fix ex = External fixation. Nail+Therapy = intramedullary nail with combined complement 5/cluster of differentiation 14 (C5/CD14) inhibitor treatment. * $p<0.05$, ** $p<0.01$, ***$p<0.001$. Sham: n = 6, Nail: n = 7, Fix ex: n = 8, Nail+Therapy: n = 4.

4 Discussion

In order to investigate the pathogenesis of trauma haemorrhage, to find appropriate medical treatment to slow down the progression of trauma haemorrhage, to reduce the mortality rate of trauma haemorrhage patients, to investigate the pathogenesis in depth and to find more effective targets for resuscitation treatment, there is an urgent need to establish a suitable model of trauma haemorrhage for research. Although there is a gap between animal models and clinical patients, the establishment of clinically relevant animal models will facilitate the understanding of the disease, and various drugs and newer methods of current clinical treatment can be validated in animal experiments beforehand.

There have been many approaches for the development of animal models of trauma haemorrhage in basic research. The method of preparing a porcine trauma blood loss model for fractures combined with blood loss due to multiple injuries is well established, and by controlling the amount of blood loss to maintain hemodynamic stability in pigs, a more consistent animal model can be obtained. Most importantly, this model is rather close to the clinical reality and its findings are therefore important for the subsequent development of animal medicine to clinical medicine (translational medicine). In addition, this model can be used to investigate the mechanisms by which the immune system functions after injury and to explore the effects of the crosstalk between multiple organs.

However, the challenge of this experimental model are to accurately control blood loss in pigs during haemorrhagic shock simulation, to avoid complications such as respiratory failure when constructing a lung contusion model, and to prevent complications such as vascular embolism in the case of bilateral lower limb femoral fractures.

The drug given in this experiment was RA101295 (2-kDa peptide) while is a broad-spectrum C5 inhibitor. The drug is characterised by blocking the cleavage of C5 and the subsequent formation of C5a and terminal C5b-9 complement complexes, the latter two in two forms: sC5b-9 in the liquid phase and the membrane attack complex (MAC) on the cell surface. C5a is an anaphylatoxin that amplifies leukocyte activation and migration, causes basophil/mast cell degranulation, enhances vascular permeability, and promotes vasoconstriction [120]. Inhibition of both C5 and C5aR significantly improves IRI in the liver, characterised by inhibition of platelet aggregation in the hepatic microcirculation and HMGB-1 release in the early stages of reperfusion. It also inhibited hepatocyte apoptosis by downregulating infiltrating macrophages and neutrophils, cytokine and chemokine release, and ROS production [72]. Blockade of either C5aR or C5 has been shown to improve hepatic IRI damage in numerous studies. In an experiment to demonstrate that C5aR antagonists inhibit local and remote organ damage after lower limb ischemia/reperfusion (I/R) in rats, it was found that LDH, ALT and AST were reduced to varying degrees after the application of C5aR antagonists indicating a key role for C5a in the induction of local and remote organ damage [161]. During liver injury, C5a mediates the activation and migration of leukocytes, ultimately leading to necrosis and apoptosis of hepatocytes. C5b and MAC lyse target cells, promoting the release of injury-associated molecular patterns, chemokines and other cytotoxins [72]. In this study we figured out that combined blockade of C5 and CD14 early in the course of injury and real-time dose adjustment during monitoring significantly reduced organ damage [82]. In this experiment, we found that the ALT and AST in each group tended to increase before 48 hours and then decreased significantly in all groups. However, a significant decrease could be seen in the Nail+Therapy group after the application of the combined immunosuppressant, which represents a novel finding.

AST and ALT are two of the most convenient and commonly used enzymatic indicators for clinical testing of liver damage. The difference in serum AST levels in

the sham group compared to the immunotherapy group at all time points was not statistically significant ($p>0.05$), indicating some improvement in hepatocyte damage after C5/CD14 immunosuppressive therapy, which was matched by the statistical results from the hepatocyte damage score.

Serum ALT levels are the most frequent and reliable indicator of hepatotoxic effects. AST to some extent more accurately reflects the severity of hepatocyte damage and necrosis than AST, as ALT is mainly distributed in the liver [98]. ALT levels in the group, which received internal fixation, increased after the onset of trauma, and total ALT levels in the Nail+Therapy group, which received C5/CD14 immunosuppressive therapy, were also higher and consistently higher than in the sham group. In our study, we found that AST rose more significantly than ALT. Michi et al. found that high serum AST was common in older underweight individuals and may reflect some skeletal muscle pathology [133]. The reason for this may be related to the fact that nailing after bilateral lower limb femur fracture may induce remote liver damage. Of note, ALT levels in case of Nail+Therapy appeared significantly lower and thus may reflect some therapeutic effects.

It is well known that a severe traumatic is a huge challenge to the various defence systems of the host. Fractures of the femur with subsequent fracture fixation can cause acute respiratory distress syndrome and multi-organ dysfunction syndrome. The causes are mainly due to the overshooting release of various pro-inflammatory cytokines -cytokine storm - including interleukin 6 [47]. Interleukin 6 (IL-6) is an interleukin that acts as both a pro-inflammatory cytokine and an anti-inflammatory factor. The increasing of IL-17A secretion by NK cells was found after liver IRI, with a concomitant increase in IL-6 levels [37]. IL-10 is one of the cytokines. It can down-regulate the expression of Th1 cytokines, MHC class II antigens and co-stimulatory molecules on macrophages during inflammation, thus acting mainly as

an anti-inflammatory agent [32]. An increase in regulatory T cells has been used to suppress innate immunity, resulting in increased levels of IL-10 [165]. The increased level of IL-10 represents a strong anti-inflammatory activity in the body. By implementing combined C5/CD14 immunosuppression, we observed a decrease of the mRNA expression of IL-10 as well as IL-6 in liver tissue of the Nail+Therapy group compared to the Nail group alone, indicating a regulatory effect of the inflammation response which might have a positive. Interleukin 2 (IL-2) is a key regulator of the adaptive immune response, but its regulatory role is not fully understood [143]. It is generally accepted that elevated liver enzymes, such as ALT and AST, are associated with elevated IL-2 [130]. Our qPCR results showed that IL-2 mRNA levels were higher in the Nail group compared to the Nail+Therapy group. On a morphological level, we used the classical HE staining method to determine morphologic changes in the liver and determine the liver injury score. The congestion area of the traumatizes pig liver was significantly enlarged and most of the hepatocytes were vacuolated and necrotic, indicating significant hepatocyte necrosis and a severe inflammatory response in the liver tissue. After liver injury caused by multiple injuries combined with haemorrhagic shock, the necrotic hepatocytes released ALT and AST into the blood, resulting in increased serum levels of ALT and AST [39]. AST levels in pigs at initial 0 h within 48 hours of multiple injuries combined with haemorrhagic shock were not significantly increased but progressively increased by trend over time and peaked at 48 hours before slowly decreasing. Combined with the laboratory results of AST and ALT, we can propose that immunosuppressive therapy has a positive protective effect on reducing liver enzymes, reducing IRI damage in the liver and reducing the inflammatory response in the liver after trauma.

In addition, major trauma can conversely affect the delayed healing of fractures. In a rat model of severe trauma, it was demonstrated that delayed fracture healing

occurred in a surgical group with femoral osteotomy plus blunt pulmonary contusion simulation, compared to a control group with femoral osteotomy alone [112]. The acute systemic inflammatory response alters the cellular composition and cytokine expression in the haematoma, which substantially diminishes the formation of bone and the mechanical competence of the fracture callus in the later stages of healing. That is a strong inducer of posttraumatic systemic inflammation [113]. During the early inflammatory phase of fracture healing, C5aR is strongly expressed not only by immune cells, but also by osteoblasts, chondrocytes and osteoclasts in the intramembranous and chondrogenic zones throughout the fracture healing period [52].

This experiment is a study of the effect of trauma on the organism and the effect of cross-linking between liver and bone under combined C5/CD14 immunosuppressants. The analysis of the PCR results above showed that the pigs in the immunomodulation group had significantly and statistically significant lower levels of IL-6 in the liver 72h after polytrauma compared to the non-immunomodulation group. This indicates that the use of C5/CD14 immunosuppressants reduced the level of the pro-inflammatory factor IL-6 in the liver. This is coherent results with the results of HE staining and liver injury scores. In pig models of sepsis, combined C5 and CD14 inhibition treatment significantly reduced thrombotic inflammation and decreased morbidity and mortality [8].

Previous studies have shown that the inhibition of complement before the trauma has a protective effect on liver, manifested by reduction of inflammation and cell apoptosis [3, 46, 84]. The liver-bone cross talk was previously described in chronic liver diseases [154]. A recent study showed that the liver-bone axis influences the development of hepatic osteodystrophy by high levels of PP2Acα (protein phosphatase 2 A catalytic subunit α isoform) [80]. RANK/RANKL, which plays an essential role in bole remodeling, activates NF-κB (Nuclear factor kappa B) in hepatocytes [64], but whether it has a role on fracture healing/bone remodeling in

polytrauma milieu, is still unclear. In our study, we found that the levels of RANKL, RANK, OPG in the liver of the Nail group were significantly and statistically higher than Nail+Therapy group. The ratio of RANKL/OPG was also significantly higher than the rest of the group, indicating high bone remodeling activity [156]. Although PCR results showed higher gene expression of OPG and RANKL in liver samples from the Nail group than in the Nail+Therapy group, contrary to the findings in the ELISA assay. The osteoblasts can generate and cleave complement proteins. C3a and C5a have been shown to stimulate RANKL expression in osteoblasts, thereby indirectly increasing osteoclast formation [53]. A rat model of blunt thoracic injury showed that intravenous administration of a C5aR antagonist improved bone bridging at the fracture gap and accelerated and improved bone scab formation [114]. The results of these studies confirm that C5 is involved in the repair of fractures and that its absence impairs the process of bone repair. Therefore, epithelial cells of wounds can strongly express C5 [65]. A study in mice with severe blunt chest injuries combined with femur fractures showed that complement activation adversely affected fracture healing. This negative effect could be reversed by systemic blockade of C5a-C5aR interactions [113]. To further investigate which role complement plays in bone development, researchers investigated fracture healing in mice lacking the key complement molecules C3 and C5. Fracture healing was found to be sufficient after 21 days in mice knocked out of C3, while fracture repair was significantly reduced in mice knocked out of C5. In addition they further demonstrated that C5a was activated in knockout C3 mice, demonstrating that activation of the terminal complement cascade response may be critical for successful fracture healing [31]. Osteoblasts can locally produce complement proteins, including C3 and C5 expressed by osteoblasts [59, 121, 122] and active C5 produced by osteoclasts [53]. In addition, C3a and C5a induce osteoblasts to release inflammatory cytokines, including IL-6 and IL-8. By injecting combined C5/CD14 inhibitors into the animals, we found lower levels of IL-6 in the treated group by the experimental method of PCR, which is consistent with previous studies that injecting immunosuppressants can effectively reduce the

concentration of IL-6 in the body and attenuate the inflammatory response. It is important to note, however, that fracture repair requires also the involvement of the terminal complement complex. We did reduce the damaging effect of the inflammatory response on the organ while applying immunosuppression, but at the same time, we also inhibited the production of the complement complex. The complement (C) 1 is activated by recognition of the immune complex by the antibody isotype immunoglobulin (Ig) G or IgM, followed by cleavage of C4 and C2 by the C1s subunit. The resulting cleavage product produces C3 convertase (C4bC2a), which cleaves C3 into C3a and C3b. C3b is involved in the formation of sC5b-9 by catalyzing the C5 cleavage reaction to produce C5a and C5b, while C5b is involved in the formation of sC5b-9 which ultimately generates the tapping membrane complex [137]. Ehrnthaller et al. pointed out that complement C3 and C5 deficiency affects fracture healing, as activation of the terminal complement cascade may be essential for successful fracture healing [31]. As a result, C5a not only induces osteoblast migration, but also alters production of interleukin 6 (IL-6) of osteoblasts [53, 105]. IL-6 is considered to be a key cytokine in initiating the repair process during fracture healing [40], which may explain the lower levels of bone modifying factors observed in our study in the Nail+Therapy group compared to the nail group.

The innovation of our current study is the combined use of C5/CD14 inhibitors to study the levels of inflammation and bone modifying factors after polytrauma and observation period of 72 h. Through continuous infusion of C5 inhibitors and intermittent administration of CD14 inhibitors, we found significant reductions in organ inflammation levels in the experimental animals, not only as assessed visually by HE staining, but also on a protein level and by the PCR evaluation. It is also worth noting that while the use of complement inhibitors had a positive effect on the protection of the organ from inflammatory responses, it may also inhibit bone healing. This means that a balanced activation of complement is necessary to promote bone

regeneration, whereas over-stimulation of complement can cause detrimental effects. The balance point of complement activation needs to be further clarified. In summary, we can conclude the following:

I. Experimental polytrauma leads to generation of the bone repair modulating factors OPG, RANK, RANKL by the liver;

II. The combined inhibition of C5/CD14 resulted in some reduction of polytrauma-induced liver inflammation and reduced generation of bone repair relevant proteins by the liver;

III. The consequences of the liver-bone-axis on fracture healing needs further investigation.

5 Summary

Multiple injuries and haemorrhagic shock are often accompanied by ischaemia-reperfusion injury to the liver. Furthermore, serve trauma activates the complement and Toll-like receptor (TLR) systems driving the inflammatory response. Therefore, blocking both system by C5/CD14 inhibition seems a promising therapeutic principle. However, the effect of combined C5/CD14 inhibitors on liver inflammation and fracture healing alter severe multiple injuries and haemorrhagic shock is still unclear, and addressed in this thesis.

Therefore, a pig model of multiple injuries and haemorrhagic shock was established in a collaborative effort with the University of Aachen (The official ethical approval number was AZ 81-02.04.2020.A215). All groups except the sham group received blunt pulmonary contusion, hepatic dissection, bilateral lower limb femoral shaft fractures and haemorrhagic shock. Four experimental groups were investigated: 1) sham animals; or polytrauma and hemorrhagic shock: 2) treated with an external fixation, or 3) treated with a nail, or 4) treated with a nail plus immunomodulatory therapy (combined C5/CD14 inhibitor). Serum samples were obtained at 0 h, 1.5 h, 2.5 h, 24 h, 48 h and 72 h after completion of the multiple injuries and hemorrhagic shock, and liver samples were obtained after euthanasia of the pigs.

As results, we found significant differences in liver injury scores between the four groups. The liver injury score was significantly higher in the nail group than in the Nail plus immunomodulation or sham groups. In terms of bruising, the Nail group was significantly higher than the Nail plus immunomodulation or sham groups, but there was no difference between the immunomodulation and sham groups, suggesting that the combination of C5/CD14 inhibition improved bruising caused by ischemia/reperfusion injury in the liver. In terms of vacuolation, necrosis and inflammation, the damage in the Nail group was more severe than in the sham or Nail

plus immunomodulation groups. While in the combined therapy group the AST levels were slightly higher than in the sham group, the difference between the two groups was not statistically significant. Overall, AST increased progressively in all groups peaking at 48 hours after trauma. AST, ALT and LDH levels were lower in the Nail plus immunomodulation group than in the non-treated group, demonstrating the positive effect of the combination of C5/CD14 inhibitors on improving liver injury. The protein levels of RANK, RANKL, OPG, OCN, OPN, IL-2, IL-6, IL-10 and ALP were all higher in the Nail group than in the Nail with immunomodulation group, suggesting that bone metabolism and bone repair activity may be affected by the intervention of the combined C5/CD14 inhibitor. However, the RANKL levels measured in the liver were higher in the Nail plus immunomodulation group than in the Nail group alone , and whereas the serum RANKL levels were lower. This may be due to the depletion of RANKL in the liver in the Nail only group. However, further experiments are needed to investigate this.

In conclusion, the use of combined C5/CD14 inhibitors attenuated the effects of the inflammatory response in the liver of pigs 72 hours after multiple injuries and haemorrhagic shock and surgically treated by a femoral Nail. Nevertheless, the use of the combined immunosuppressant may also exhibit some negative effects on bone repair, which needs further evaluation.

6 Bibliography

1. Abu-Amara M, Yang SY, Tapuria N, Fuller B, Davidson B, Seifalian A: Liver ischemia/reperfusion injury: processes in inflammatory networks—a review. *Liver Transplantation* 2010; 16: 1016-1032.

2. Ahmad T, Thapaliya P, Dawani S, Sikander N, Mazcuri M: Morbidity and mortality among patients sustaining chest injury due to blunt force–the difference between young and elderly. *Journal of Ayub Medical College Abbottabad* 2020; 32: 512-516.

3. Arumugam TV, Woodruff TM, Stocks SZ, Proctor LM, Pollitt S, Shiels IA, et al.: Protective effect of a human C5a receptor antagonist against hepatic ischaemia-reperfusion injury in rats. *Journal of hepatology* 2004; 40: 934-941.

4. Ashbaugh D, Bigelow DB, Petty T, Levine B: Acute respiratory distress in adults. *The Lancet* 1967; 290: 319-323.

5. Aufmkolk M, Majetschak M, Voggenreiter G, Obertacke U, Schmit-Neuerburg K: Follow-up and prognosis of severe accidental trauma in the aged. *Der Unfallchirurg* 1997; 100: 477-482.

6. Badger S, Barclay R, Campbell P, Mole D, Diamond T: Management of liver trauma. *World journal of surgery* 2009; 33: 2522-2537.

7. Bao F, Bailey CS, Gurr KR, Bailey SI, Rosas-Arellano MP, Dekaban GA, et al.: Increased oxidative activity in human blood neutrophils and monocytes after spinal cord injury. *Experimental neurology* 2009; 215: 308-316.

8. Barratt-Due A, Thorgersen EB, Egge K, Pischke S, Sokolov A, Hellerud BC, et al.: Combined inhibition of complement (C5) and CD14 markedly attenuates blood thrombogenicity, inflammation and hemodynamic changes in porcine sepsis. *Immunobiology* 2012; 11: 819-827.

9. Bastian O, Pillay J, Alblas J, Leenen L, Koenderman L, Blokhuis T: Systemic inflammation and fracture healing. *Journal of leukocyte biology* 2011; 89: 669-673.

10. Bigford GE, Bracchi-Ricard VC, Keane RW, Nash MS, Bethea JR: Neuroendocrine and cardiac metabolic dysfunction and NLRP3 inflammasome activation in adipose tissue and pancreas following chronic spinal cord injury in the mouse. *ASN neuro* 2013; 5: 243-255.

11. Bigford GE, Bracchi-Ricard VC, Nash MS, Bethea JR: Alterations in mouse hypothalamic adipokine gene expression and leptin signaling following chronic spinal cord injury and with advanced age. *PLoS One* 2012; 7: e41073.

12. Boury NM, Czuprynski CJ: Listeria monocytogenes infection increases neutrophil adhesion and damage to a murine hepatocyte cell line in vitro. *Immunology letters* 1995; 46: 111-116.

13. Brooke HL, Talbäck M, Hörnblad J, Johansson LA, Ludvigsson JF, Druid H, et al.: The Swedish cause of death register. *European journal of epidemiology* 2017; 32: 765-773.

14. Bystrom P, Foley N, Toledo-Pereyra L, Quesnelle K: Ischemic preconditioning modulates ROS to confer protection in liver ischemia and reperfusion. *EXCLI journal* 2017; 16: 483-496.

15. Cannistrà M, Ruggiero M, Zullo A, Gallelli G, Serafini S, Maria M, et al.: Hepatic ischemia reperfusion injury: A systematic review of literature and the role of current drugs and biomarkers. *International Journal of Surgery* 2016; 33: 57-70.

16. Chai YS, Lee JK, Heo SJ, Lee YK, Lee YW, Jo YH, et al.: Traumatic Liver Injury: Factors Associated with Mortality. *Korean Journal of Critical Care Medicine* 2014; 29: 320-327.

17. Chang WJ, Toledo-Pereyra LH: Toll-like receptor signaling in liver ischemia and reperfusion. *Journal of Investigative Surgery* 2012; 25: 271-277.

18. Ciechanowicz D, Samojło N, Kozłowski J, Pakulski C, Żyluk A: Incidence and etiology of mortality in polytrauma patients: an analysis of material from Multitrauma Centre of the University Teaching Hospital no 1 in Szczecin, over a period of 3 years (2017–2019). *Polish Journal of Surgery* 2020; 92: 1-6.

19. Cohick W, Clemmons D: The insulin-like growth factors. *Annual review of physiology* 1993; 55: 131-153.

20. Colombo F, Sansonna F, Baticci F, Corso R, Scandroglio I, Maggioni D, et al.: Liver trauma: experience in the management of 252 cases. *Chirurgia italiana* 2005; 57: 695-702.

21. Cursio R, Colosetti P, Gugenheim J: Autophagy and liver ischemia-reperfusion injury. *BioMed research international* 2015; 2015: 417590

22. Cutrn JC, Perrelli M-G, Cavalieri B, Peralta C, Catafau JR, Poli G: Microvascular dysfunction induced by reperfusion injury and protective effect of ischemic preconditioning. *Free Radical Biology and Medicine* 2002; 33: 1200-1208.

23. Czigany Z, Lurje I, Schmelzle M, Schöning W, Öllinger R, Raschzok N, et al.: Ischemia-Reperfusion Injury in Marginal Liver Grafts and the Role of Hypothermic Machine Perfusion: Molecular Mechanisms and Clinical Implications. *Journal of Clinical Medicine* 2020; 9: 846-863.

24. Dąbrowski W, Nestorowicz A, Wośko J, Zadora P, Tomaszewski A, Jurko C: Tricuspidal valve rupture after blunt chest trauma. *Anestezjologia intensywna terapia* 2011; 43: 239-243.

25. Datta G, Fuller BJ, Davidson BR: Molecular mechanisms of liver ischemia reperfusion injury: insights from transgenic knockout models. *World journal of gastroenterology: WJG* 2013; 19: 1683-1698.

26. Daurat A, Millet I, Roustan J-P, Maury C, Taourel P, Jaber S, et al.: Thoracic Trauma Severity score on admission allows to determine the risk of delayed ARDS in trauma patients with pulmonary contusion. *Injury* 2016; 47: 147-153.

27. DeMaria M, Kaplan J, Baik J-J: Upper-level eddy angular momentum fluxes and tropical cyclone intensity change. *Journal of Atmospheric Sciences* 1993; 50: 1133-1147.

28. Denis-Aubrée P, Dukan R, Karam K, Molina V, Court C, Bouthors C: Bilateral femoral shaft fracture in polytrauma patients: Can intramedullary nailing be done on an emergency basis? *Orthopaedics & Traumatology: Surgery & Research* 2021; 107: 102864.

29. Duvigneau JC, Kozlov AV, Zifko C, Postl A, Hartl RT, Miller I, et al.: Reperfusion does not induce oxidative stress but sustained endoplasmic reticulum stress in livers of rats subjected to traumatic-hemorrhagic shock. *Shock* 2010; 33: 289-298.

30. Dziodzio T, Biebl M, Pratschke J: Impact of brain death on ischemia/reperfusion injury in liver transplantation. *Current opinion in organ transplantation* 2014; 19: 108-114.

31. Ehrnthaller C, Huber-Lang M, Nilsson P, Bindl R, Redeker S, Recknagel S, et al.: Complement C3 and C5 deficiency affects fracture healing. *PloS one* 2013; 8: e81341.

32. Eskdale J, Kube D, Tesch H, Gallagher G: Mapping of the human IL10 gene and further characterization of the 5'flanking sequence. *Immunogenetics* 1997; 46: 120-128.

33. Evans JA, van Wessem KJ, McDougall D, Lee KA, Lyons T, Balogh ZJ: Epidemiology of traumatic deaths: comprehensive population-based assessment. *World journal of surgery* 2010; 34: 158-163.

34. Faist E, Baue A, Dittmer H, Heberer G: Multiple organ failure in polytrauma patients. *The*

Journal of trauma 1983; 23: 775-787.

35. Fakhry SM, Rutledge R, Dahners LE, Kessler D: Incidence, management, and outcome of femoral shaft fracture: a statewide population-based analysis of 2805 adult patients in a rural state. *The Journal of trauma* 1994; 37: 255-260.

36. Favre PA, de Molliens L, Petit L, Biais M, Carrié C: May the neutrophil-to-lymphocyte ratio at admission predict the occurrence and the severity of ARDS after blunt chest trauma patients? A retrospective study. *The American Journal of Emergency Medicine* 2021; 39: 137-142.

37. Feng M, Li G, Qian X, Fan Y, Huang X, Zhang F, et al.: IL-17A-producing NK cells were implicated in liver injury induced by ischemia and reperfusion. *International immunopharmacology* 2012; 13: 135-140.

38. Fernández AR, Sánchez-Tarjuelo R, Cravedi P, Ochando J, López-Hoyos M: Ischemia Reperfusion Injury—A Translational Perspective in Organ Transplantation. *International Journal of Molecular Sciences* 2020; 21: 8549.

39. Fox A, Sanderlin JB, McNamee S, Bajaj JS, Carne W, Cifu DX: Elevated liver enzymes following polytraumatic injury. *Journal of Rehabilitation Research and Development* 2014; 51: 869-874.

40. Gerstenfeld LC, Cho TJ, Kon T, Aizawa T, Tsay A, Fitch J, et al.: Impaired fracture healing in the absence of TNF-α signaling: The role of TNF-α in endochondral cartilage resorption. *Journal of Bone and Mineral Research* 2003; 18: 1584-1592.

41. Giffen PS, Pick CR, Price MA, Williams A, York MJ: Alpha-glutathione S-transferase in the assessment of hepatotoxicity—its diagnostic utility in comparison with other recognized markers in the Wistar Han rat. *Toxicologic pathology* 2002; 30: 365-372.

42. Ginès P, Guevara M, Arroyo V, Rodés J: Hepatorenal syndrome. *The Lancet* 2003; 362: 1819-1827.

43. Gong T, Liu L, Jiang W, Zhou R: DAMP-sensing receptors in sterile inflammation and inflammatory diseases. *Nature Reviews Immunology* 2020; 20: 95-112.

44. Guan L-Y, Fu P-Y, Li P-D, Li Z-N, Liu H-Y, Xin M-G, et al.: Mechanisms of hepatic ischemia-reperfusion injury and protective effects of nitric oxide. *World journal of gastrointestinal surgery* 2014; 6: 122-128.

45. Haagsma JA, Graetz N, Bolliger I, Naghavi M, Higashi H, Mullany EC, et al.: The global burden of injury: incidence, mortality, disability-adjusted life years and time trends from the Global Burden of Disease study 2013. *Injury prevention* 2016; 22: 3-18.

46. He S, Atkinson C, Qiao F, Cianflone K, Chen X, Tomlinson S: A complement-dependent balance between hepatic ischemia/reperfusion injury and liver regeneration in mice. *The Journal of clinical investigation* 2009; 119: 2304-2316.

47. Heeres M, Visser T, van Wessem KJ, Koenderman AH, Strengers PF, Koenderman L, et al.: The effect of C1-esterase inhibitor on systemic inflammation in trauma patients with a femur fracture-The CAESAR study: study protocol for a randomized controlled trial. *Trials* 2011; 12: 1-6.

48. Horst K, Greven J, Lüken H, Zhi Q, Pfeifer R, Simon TP, et al.: Trauma Severity and Its Impact on Local Inflammation in Extremity Injury—Insights From a Combined Trauma Model in Pigs. *Frontiers in immunology* 2020; 10: 3028.

49. Huang J, Xie P, Dong Y, An W: Inhibition of Drp1 SUMOylation by ALR protects the liver from ischemia-reperfusion injury. *Cell Death & Differentiation* 2021; 28: 1174-1192.

50. Huber-Lang M, Lambris JD, Ward PA: Innate immune responses to trauma. *Nature immunology* 2018; 19: 327-341.

51. Huber-Lang MS, Ignatius A, Köhl J, Mannes M, Braun CK: Complement in trauma—Traumatised complement? *British Journal of Pharmacology* 2021; 178: 2863-2879.

52. Ignatius A, Ehrnthaller C, Brenner RE, Kreja L, Schoengraf P, Lisson P, et al.: The anaphylatoxin receptor C5aR is present during fracture healing in rats and mediates osteoblast migration in vitro. *The Journal of trauma* 2011; 71: 952-960.

53. Ignatius A, Schoengraf P, Kreja L, Liedert A, Recknagel S, Kandert S, et al.: Complement C3a and C5a modulate osteoclast formation and inflammatory response of osteoblasts in synergism with IL-1β. *Journal of cellular biochemistry* 2011; 112: 2594-2605.

54. Ikeda T, Yanaga K, Kishikawa K, Kakizoe S, Shimada M, Sugimachi K: Ischemic injury in liver transplantation: difference in injury sites between warm and cold ischemia in rats. *Hepatology* 1992; 16: 454-461.

55. Ito T, Naini BV, Markovic D, Aziz A, Younan S, Lu M, et al.: Ischemia-reperfusion injury and its relationship with early allograft dysfunction in liver transplant patients. *American Journal of Transplantation* 2021; 21: 614-625.

56. Jaeschke H: Mechanisms of neutrophil-induced liver cell injury during hepatic ischemia-reperfusion and other acute inflammatory conditions. *Am J Physiol Gas-trointest Liver Physiol* 2006; 290: 1083-1088.

57. Jarrar D, Chaudry IH, Wang P: Organ dysfunction following hemorrhage and sepsis: mechanisms and therapeutic approaches. *International journal of molecular medicine* 1999; 4: 575-658.

58. Jastrow III KM, Gonzalez EA, McGuire MF, Suliburk JW, Kozar RA, Iyengar S, et al.: Early cytokine production risk stratifies trauma patients for multiple organ failure. *Journal of the American College of Surgeons* 2009; 209: 320-331.

59. Jin CH, Shinki T, Hong M, Sato T, Yamaguchi A, Ikeda T, et al.: 1 alpha, 25-dihydroxyvitamin D3 regulates in vivo production of the third component of complement (C3) in bone. *Endocrinology* 1992; 131: 2468-2475.

60. Kamdar K, Nguyen V, DePaolo RW: Toll-like receptor signaling and regulation of intestinal immunity. *Virulence* 2013; 4: 207-212.

61. Kamei H, Yoshida S, Yamasaki K, Tajiri T, Ozaki K, Shirouzu K: Severity of trauma changes expression of TNF-α mRNA in the brain of mice. *Journal of Surgical Research* 2000; 89: 20-25.

62. Keller P: Enzyme activities in the dog: tissue analyses, plasma values, and intracellular distribution. *American Journal of Veterinary Research* 1981; 42: 575-582.

63. Kepp O, Senovilla L, Vitale I, Vacchelli E, Adjemian S, Agostinis P, et al.: Consensus guidelines for the detection of immunogenic cell death. *Oncoimmunology* 2014; 3: e955691.

64. Kiechl S, Wittmann J, Giaccari A, Knoflach M, Willeit P, Bozec A, et al.: Blockade of receptor activator of nuclear factor-κB (RANKL) signaling improves hepatic insulin resistance and prevents development of diabetes mellitus. *Nature medicine* 2013; 19: 358-363.

65. Kimura Y, Madhavan M, Call MK, Santiago W, Tsonis PA, Lambris JD, et al.: Expression of complement 3 and complement 5 in newt limb and lens regeneration. *The Journal of Immunology* 2003; 170: 2331-2339.

66. Kini U, Nandeesh B. Physiology of bone formation, remodeling, and metabolism. *Radionuclide and hybrid bone imaging: Springer* 2012; 2012: 29-57.

67. Kleber C, Giesecke MT, Tsokos M, Haas NP, Schaser KD, Stefan P, et al.: Overall distribution of trauma-related deaths in Berlin 2010: advancement or stagnation of German trauma management? *World journal of surgery* 2012; 36: 2125-2130.

68. Klune JR, Tsung A: Molecular biology of liver ischemia/reperfusion injury: established mechanisms and recent advancements. *Surgical Clinics* 2010; 90: 665-677.

69. Kobbe P, Vodovotz Y, Kaczorowski DJ, Mollen KP, Billiar TR, Pape H-C: Patterns of cytokine release and evolution of remote organ dysfunction after bilateral femur fracture. *Shock* 2008; 30: 43-47.

70. Konishi T, Lentsch AB: Hepatic ischemia/reperfusion: mechanisms of tissue injury, repair, and regeneration. *Gene expression* 2017; 17: 277-287.

71. Kubes P, Mehal WZ: Sterile inflammation in the liver. *Gastroenterology* 2012; 143: 1158-1172.

72. Kusakabe J, Hata K, Tamaki I, Tajima T, Miyauchi H, Wang Y, et al.: Complement 5 inhibition ameliorates hepatic ischemia/reperfusion injury in mice, dominantly via the C5a-mediated cascade. *Transplantation* 2020; 104: 2065-2077.

73. Langdale LA, Hoagland V, Benz W, Riehle KJ, Campbell JS, Liggitt DH, et al.: Suppressor of cytokine signaling expression with increasing severity of murine hepatic ischemia-reperfusion injury. *Journal of hepatology* 2008; 49: 198-206.

74. Lashoher A, Schneider EB, Juillard C, Stevens K, Colantuoni E, Berry WR, et al.: Implementation of the World Health Organization Trauma Care Checklist Program in 11 centers across multiple economic strata: effect on care process measures. *World journal of surgery* 2017; 41: 954-962.

75. Lee SM, Hutchinson M, Saint DA: The role of Toll-like receptor 4 (TLR4) in cardiac ischaemic-reperfusion injury, cardioprotection and preconditioning. *Clinical and Experimental Pharmacology and Physiology* 2016; 43: 864-871.

76. Lentsch AB, Yoshidome H, Cheadle WG, Miller FN, Edwards MJ: Chemokine involvement in hepatic ischemia/reperfusion injury in mice: roles for macrophage inflammatory protein-2 and Kupffer cells. *Hepatology* 1998; 27: 507-512.

77. Liakopoulos OJ, Ho JK, Yezbick A, Sanchez E, Naddell C, Buckberg GD, et al.: An experimental and clinical evaluation of a novel central venous catheter with integrated oximetry for pediatric patients undergoing cardiac surgery. *Anesthesia & Analgesia* 2007; 105: 1598-1604.

78. Lindblom P, Rafter I, Copley C, Andersson U, Hedberg JJ, Berg A-L, et al.: Isoforms of alanine aminotransferases in human tissues and serum—differential tissue expression using novel antibodies. *Archives of biochemistry and biophysics* 2007; 466: 66-77.

79. Liu Y, Lu T, Zhang C, Xu J, Xue Z, Busuttil RW, et al.: Activation of YAP attenuates hepatic damage and fibrosis in liver ischemia-reperfusion injury. *Journal of hepatology* 2019; 71: 719-730.

80. Lu K, Shi T-S, Shen S-Y, Shi Y, Gao H-L, Wu J, et al.: Defects in a liver-bone axis contribute to hepatic osteodystrophy disease progression. *Cell Metabolism* 2022; 34: 441-457.

81. Lu L, Zhou H, Ni M, Wang X, Busuttil R, Kupiec-Weglinski J, et al.: Innate immune regulations and liver ischemia reperfusion injury. *Transplantation* 2016; 100: 2601-2610.

82. Lupu L, Horst K, Greven J, Mert Ü, Ludviksen JA, Pettersen K, et al.: Simultaneous C5 and CD14 inhibition limits inflammation and organ dysfunction in pig polytrauma. *Frontiers in Immunology* 2022; 13: 952267.

83. Mahmood I, El-Menyar A, Younis B, Ahmed K, Nabir S, Ahmed MN, et al.: Clinical significance and prognostic implications of quantifying pulmonary contusion volume in patients with blunt chest trauma. *Medical science monitor: international medical journal of experimental and clinical research* 2017; 23: 3641-3648.

84. Marshall KM, He S, Zhong Z, Atkinson C, Tomlinson S: Dissecting the complement pathway in hepatic injury and regeneration with a novel protective strategy. *Journal of Experimental Medicine* 2014; 211: 1793-1805.

85. Martins RM, Teodoro JS, Furtado E, Rolo AP, Palmeira CM, Tralhão JG: Recent insights into mitochondrial targeting strategies in liver transplantation. *International journal of medical sciences* 2018; 15: 248-256.

86. Masiukiewicz US, Mitnick M, Grey AB, Insogna KL: Estrogen modulates parathyroid hormone-induced interleukin-6 production in vivo and in vitro. *Endocrinology* 2000; 141: 2526-2531.

87. Matzinger P: Tolerance, danger, and the extended family. *Annual review of immunology* 1994; 12:991-1045.

88. McGhan LJ, Jaroszewski DE: The role of toll-like receptor-4 in the development of multi-organ failure following traumatic haemorrhagic shock and resuscitation. *Injury* 2012; 43: 129-136.

89. Miller C, Stolarski A, Ata A, Pfaff A, Nadendla P, Owens K, et al.: Impact of blunt pulmonary contusion in polytrauma patients with rib fractures. *The American Journal of Surgery* 2019; 218:51-55.

90. Mirzayan M, Probst C, Samii M, Krettek C, Gharabaghi A, Pape H, et al.: Histopathological features of the brain, liver, kidney and spleen following an innovative polytrauma model of the mouse. *Experimental and toxicologic pathology* 2012; 64: 133-139.

91. Moore Ernest E, Cogbill Thomas H, Jurkovich Gregory J, Shackford Steven R, Malangoni Mark A, Champion Howard R: Organ injury scaling: spleen and liver. *J Trauma Injury Infect Critical Care* 1995; 38: 323-324.

92. Moran A, Arikan AA, Mastrangelo M-AA, Wu Y, Yu B, Poli V, et al.: Prevention of trauma and hemorrhagic shock-mediated liver apoptosis by activation of stat3α. *International journal of clinical and experimental medicine* 2008; 1: 213-247.

93. Nagendra AR, Mickelson JK, Smith C: CD18 integrin and CD54-dependent neutrophil adhesion to cytokine-stimulated human hepatocytes. *American Journal of Physiology-Gastrointestinal and Liver Physiology* 1997; 272: 408-416.

94. Nakano Y, Kondo T, Matsuo R, Murata S, Fukunaga K, Ohkohchi N: Prevention of leukocyte activation by the neutrophil elastase inhibitor, sivelestat, in the hepatic microcirculation after ischemia-reperfusion. *Journal of Surgical Research* 2009; 155: 311-317.

95. Nakchbandi IA: Osteoporosis and fractures in liver disease: relevance, pathogenesis and therapeutic implications. *World journal of gastroenterology: WJG* 2014; 20: 9427-9438.

96. Nast-Kolb D, Aufmkolk M, Rucholtz S, Obertacke U, Waydhas C: Multiple organ failure still a major cause of morbidity but not mortality in blunt multiple trauma. *Journal of Trauma and Acute Care Surgery* 2001; 51: 835-842.

97. Nastos C, Kalimeris K, Papoutsidakis N, Tasoulis M-K, Lykoudis PM, Theodoraki K, et al.: Global consequences of liver ischemia/reperfusion injury. *Oxidative medicine and cellular longevity* 2014; 2014: 906965

98. Nathwani RA, Pais S, Reynolds TB, Kaplowitz N: Serum alanine aminotransferase in skeletal muscle diseases. *Hepatology* 2005; 41: 380-382.

99. Negoi I, Paun S, Hostiuc S, Stoica B, Tanase I, Negoi RI, et al.: Mortality after acute trauma: Progressive decreasing rather than a trimodal distribution. *Journal of Acute Disease* 2015; 4: 205-209.

100. Olthof PB, Reiniers MJ, Dirkes MC, van Gulik TM, Heger M, van Golen RF: Protective mechanisms of hypothermia in liver surgery and transplantation. *Molecular Medicine* 2015; 21: 833-846.

101. Oppenheimer L, Craven K, Forkert L, Wood L: Pathophysiology of pulmonary contusion in dogs. *Journal of Applied Physiology* 1979; 47: 718-728.

102. Paffrath T, Lefering R, Flohé S, DGU T: How to define severely injured patients?—An Injury

Severity Score (ISS) based approach alone is not sufficient. *Injury* 2014; 45: 64-69.

103. Parray FQ, Wani ML, Malik AA, Thakur N, Wani RA, Naqash SH, et al.: Evaluating a conservative approach to managing liver injuries in Kashmir, India. *Journal of Emergencies, Trauma and Shock* 2011; 4: 483-487.

104. Pfeifer R, Heussen N, Michalewicz E, Hilgers R-D, Pape H-C: Incidence of adult respiratory distress syndrome in trauma patients: a systematic review and meta-analysis over a period of three decades. *Journal of Trauma and Acute Care Surgery* 2017; 83: 496-506.

105. Pobanz JM, Reinhardt RA, Koka S, Sanderson SD: C5a modulation of interleukin-1β-induced interleukin-6 production by human osteoblast-like cells. *Journal of periodontal research* 2000; 35: 137-145.

106. Poletti PA, Mirvis SE, Shanmuganathan K, Killeen KL, Coldwell D: CT criteria for management of blunt liver trauma: correlation with angiographic and surgical findings. *Radiology* 2000; 216: 418-427.

107. Popovich PG, Stuckman S, Gienapp IE, Whitacre CC: Alterations in immune cell phenotype and function after experimental spinal cord injury. *Journal of neurotrauma* 2001; 18: 957-966.

108. Portella A, Montero E, de Figueiredo LP, Bueno A, Thurow A, Rodrigues F, editors. Effects of N-acetylcysteine in hepatic ischemia-reperfusion injury during hemorrhagic shock. Transplantation proceedings 2004; 36: 846-848.

109. Probst C, Pape H-C, Hildebrand F, Regel G, Mahlke L, Giannoudis P, et al.: 30 years of polytrauma care: an analysis of the change in strategies and results of 4849 cases treated at a single institution. *Injury* 2009; 40: 77-83.

110. Qiao Y-l, Qian J-m, Wang F-r, Ma Z-y, Wang Q-w: Butyrate protects liver against ischemia reperfusion injury by inhibiting nuclear factor kappa B activation in Kupffer cells. *Journal of Surgical Research* 2014; 187:653- 659.

111. Qin C-C, Liu Y-N, Hu Y, Yang Y, Chen Z: Macrophage inflammatory protein-2 as mediator of inflammation in acute liver injury. *World journal of gastroenterology* 2017; 23: 3043-3052.

112. Recknagel S, Bindl R, Brochhausen C, Göckelmann M, Wehner T, Schoengraf P, et al.: Systemic inflammation induced by a thoracic trauma alters the cellular composition of the early fracture callus. *Journal of Trauma and Acute Care Surgery* 2013; 74: 531-537.

113. Recknagel S, Bindl R, Kurz J, Wehner T, Ehrnthaller C, Knöferl MW, et al.: Experimental blunt chest trauma impairs fracture healing in rats. *Journal of Orthopaedic Research* 2011; 29: 734-739.

114. Recknagel S, Bindl R, Kurz J, Wehner T, Schoengraf P, Ehrnthaller C, et al.: C5aR-antagonist significantly reduces the deleterious effect of a blunt chest trauma on fracture healing. *Journal of Orthopaedic Research* 2012; 30: 581-586.

115. Regel G, Lobenhoffer P, Grotz M, Pape H, Lehmann U, Tscherne H: Treatment results of patients with multiple trauma: an analysis of 3406 cases treated between 1972 and 1991 at a German Level I Trauma Center. *Journal of Trauma and Acute Care Surgery* 1995; 38: 70-78.

116. Rowell SE, Meier EN, McKnight B, Kannas D, May S, Sheehan K, et al.: Effect of out-of-hospital tranexamic acid vs placebo on 6-month functional neurologic outcomes in patients with moderate or severe traumatic brain injury. *Jama* 2020; 324: 961-974.

117. Saam Morshed CM, Miclau III T: Suppl 1: M8: Timing of Femoral Shaft Fracture Fixation Affects Length of Hospital Stay in Patients with Multiple Injuries. *The open orthopaedics journal* 2015; 9: 324-331.

118. Sailhamer EA, Li Y, Smith EJ, Liu B, Shuja F, Soupir CP, et al.: Hypoxic “second hit” in

leukocytes from trauma patients: modulation of the immune response by histone deacetylase inhibition. *Cytokine* 2010; 49: 303-311.

119. Sakr Y, Dubois M-J, De Backer D, Creteur J, Vincent J-L: Persistent microcirculatory alterations are associated with organ failure and death in patients with septic shock. *Critical care medicine* 2004; 32: 1825-1831.

120. Sarma JV, Ward PA: New developments in C5a receptor signaling. *Cell health and cytoskeleton* 2012; 4: 73-82.

121. Sato T, Abe E, Jin CH, Hong M, Katagiri T, Kinoshita T, et al.: The biological roles of the third component of complement in osteoclast formation. *Endocrinology* 1993; 133: 397-404.

122. Sato T, Hong MH, Jin CH, Ishimi Y, Udagawa N, Shinki T, et al.: The specific production of the third component of complement by osteoblastic cells treated with 1α, 25-dihydroxyvitamin D3. *FEBS letters* 1991; 285: 21-24.

123. Sauaia A, Moore EE, Johnson JL, Chin TL, Banerjee A, Sperry JL, et al.: Temporal trends of postinjury multiple-organ failure: still resource intensive, morbid, and lethal. *The journal of trauma and acute care surgery* 2014; 76: 582-592.

124. Sauaia A, Moore FA, Moore EE, Moser KS, Brennan R, Read RA, et al.: Epidemiology of trauma deaths: a reassessment. *Journal of Trauma and Acute Care Surgery* 1995; 38: 185-193.

125. Schmieg Jr RE, Tinsley KW, Swanson PE, Karl IE, Aft R, Buchman TG, et al.: Rapid onset of hepatocyte apoptosis in a patient with trauma. *Journal of Trauma and Acute Care Surgery* 2000; 49: 542-546.

126. Seeto RK, Fenn B, Rockey DC: Ischemic hepatitis: clinical presentation and pathogenesis. *The American journal of medicine* 2000; 109: 109-113.

127. Segura-Sampedro JJ, Pineño-Flores C, Craus-Miguel A, Morales-Soriano R, González-Argente FX: New hemostatic device for grade IV–V liver injury in porcine model: a proof of concept. *World Journal of Emergency Surgery* 2019; 14: 58.

128. Seki E, Schwabe RF: Hepatic inflammation and fibrosis: functional links and key pathways. *Hepatology* 2015; 61: 1066-1079.

129. Selzner M, RüDiger HA, Sindram D, Madden J, Clavien P-A: Mechanisms of ischemic injury are different in the steatotic and normal rat liver. *Hepatology* 2000; 32: 1280-1098.

130. Senaratne T, Carr J, Noordeen F: Elevation in liver enzymes is associated with increased IL-2 and predicts severe outcomes in clinically apparent dengue virus infection. *Cytokine* 2016; 83: 182-188.

131. Sharma OP, Oswanski MF, Stringfellow KC, Raj SS: Pediatric blunt trauma: a retrospective analysis in a level I trauma center. *The American Surgeon* 2006; 72: 538-543.

132. Shenkman B, Budnik I, Einav Y, Hauschner H, Andrejchin M, Martinowitz U: Model of trauma-induced coagulopathy including hemodilution, fibrinolysis, acidosis, and hypothermia: Impact on blood coagulation and platelet function. *Journal of Trauma and Acute Care Surgery* 2017; 82: 287-292.

133. Shibata M, Nakajima K, Higuchi R, Iwane T, Sugiyama M, Nakamura T: High concentration of serum aspartate aminotransferase in older underweight people: results of the Kanagawa Investigation of the Total Check-Up Data from the National Database-2 (KITCHEN-2). *Journal of clinical medicine* 2019; 8: 1282-1292.

134. Shorr RM, Crittenden M, Indeck M, Hartunian SL, Rodriguez A: Blunt thoracic trauma. Analysis of 515 patients. *Annals of surgery* 1987; 206: 200-205.

135. Sikander N, Ahmad T, Shaikh Sr KA, Abid A, Mazcuri M, Nasreen S: Analysis of injury patterns

and outcomes of blunt thoracic trauma in elderly patients. *Cureus* 2020; 12: e9974

136. Stewart RK, Dangi A, Huang C, Murase N, Kimura S, Stolz DB, et al.: A novel mouse model of depletion of stellate cells clarifies their role in ischemia/reperfusion-and endotoxin-induced acute liver injury. *Journal of hepatology* 2014; 60: 298-305.

137. Struglics A, Okroj M, Swärd P, Frobell R, Saxne T, Lohmander LS, et al.: The complement system is activated in synovial fluid from subjects with knee injury and from patients with osteoarthritis. *Arthritis research & therapy* 2016; 18: 1-11.

138. Subhani SS, Muzaffar MS, Khan MI: Comparison of outcome between low and high thoracic trauma severity score in blunt trauma chest patients. *Journal of Ayub Medical College Abbottabad* 2014; 26: 474-477.

139. Szabo G, Romics Jr L, Frendl G: Liver in sepsis and systemic inflammatory response syndrome. *Clinics in liver disease* 2002; 6: 1045-1066.

140. Tan H, Zhao F, Hao H, Liu Z: Cost analysis of road traffic crashes in China. *International journal of injury control and safety promotion* 2020; 27: 385-391.

141. Teixeira PG, Inaba K, Hadjizacharia P, Brown C, Salim A, Rhee P, et al.: Preventable or potentially preventable mortality at a mature trauma center. *Journal of Trauma and Acute Care Surgery* 2007; 63: 1338-1347.

142. Thaiss CA, Levy M, Itav S, Elinav E: Integration of innate immune signaling. *Trends in immunology* 2016; 37: 84-101.

143. Tolksdorf F, Mikulec J, Geers B, Endig J, Sprezyna P, Heukamp LC, et al.: The PDL1-inducible GTPase Arl4d controls T effector function by limiting IL-2 production. *Scientific reports* 2018; 8: 1-9.

144. Tran DH, Sameed M, Marciniak ET, Verceles AC: Human Metapneumovirus Pneumonia Precipitating Acute Respiratory Distress Syndrome in an Adult Patient. *Cureus* 2021; 13: e16434.

145. Tselepidis S, Papazoglou L, Dessiris A, Vlemas I, Papageorgiou G, Stournara A, et al.: Liver injury after ischemia and reperfusion: the role of oxygen free radicals. *Military medicine* 2004; 169: 531-535.

146. Tsung A, Hoffman RA, Izuishi K, Critchlow ND, Nakao A, Chan MH, et al.: Hepatic ischemia/reperfusion injury involves functional TLR4 signaling in nonparenchymal cells. *The Journal of Immunology* 2005; 175: 7661-7668.

147. Tsung A, Klune JR, Zhang X, Jeyabalan G, Cao Z, Peng X, et al.: HMGB1 release induced by liver ischemia involves Toll-like receptor 4–dependent reactive oxygen species production and calcium-mediated signaling. *The Journal of experimental medicine* 2007; 204: 2913-2923.

148. Uhlen M, Oksvold P, Fagerberg L, Lundberg E, Jonasson K, Forsberg M, et al.: Towards a knowledge-based human protein atlas. *Nature biotechnology* 2010; 28: 1248-1250.

149. van Golen RF, van Gulik TM, Heger M: Mechanistic overview of reactive species-induced degradation of the endothelial glycocalyx during hepatic ischemia/reperfusion injury. *Free Radical Biology and Medicine* 2012; 52: 1382-1402.

150. van Golen RF, van Gulik TM, Heger M: The sterile immune response during hepatic ischemia/reperfusion. *Cytokine & growth factor reviews* 2012; 23: 69-84.

151. Vardanian AJ, Busuttil RW, Kupiec-Weglinski JW: Molecular mediators of liver ischemia and reperfusion injury: a brief review. *Molecular Medicine* 2008; 14: 337-345.

152. Vécsei V, Arbes S, Aldrian S, Nau T: Chest injuries in polytrauma. *European Journal of Trauma* 2005; 31: 239-243.

153. Vorobjeva N, Chernyak B: NETosis: Molecular Mechanisms, Role in Physiology and Pathology.

Biochemistry (Moscow) 2020; 85: 1178-1190.

154. Wang B, Xu H, Li J, Gao HM, Xing YH, Lin Z, et al.: Complement depletion with cobra venom factor alleviates acute hepatic injury induced by ischemia-reperfusion. *Molecular medicine reports* 2018; 18: 4523-4529.

155. Wang R, Qi Y, Wang Y, Wang Y: Characteristics of injury patients in the emergency department in Shanghai, China: a retrospective observational study. *Medical Science Monitor: International Medical Journal of Experimental and Clinical Research* 2020; 26:e922726-1.

156. Wang X-F, Zhang Y-K, Yu Z-S, Zhou J-L: The role of the serum RANKL/OPG ratio in the healing of intertrochanteric fractures in elderly patients. *Molecular medicine reports* 2013; 7: 1169-1172.

157. Wetzel G, Relja B, Klarner A, Henrich D, Dehne N, Brühne B, et al.: Myeloid knockout of HIF-1 α does not markedly affect hemorrhage/resuscitation-induced inflammation and hepatic injury. *Mediators of inflammation* 2014; 2014: 930419.

158. Wijdicks EF: Hepatic encephalopathy. *New England Journal of Medicine* 2016; 375: 1660-1670.

159. Willett K, Al-Khateeb H, Kotnis R, Bouamra O, Lecky F: Risk of mortality: the relationship with associated injuries and fracture treatment methods in patients with unilateral or bilateral femoral shaft fractures. *Journal of Trauma and Acute Care Surgery* 2010; 69: 405-410.

160. Witthaut R, Farhood A, Smith CW, Jaeschke H: Complement and tumor necrosis factor-α contribute to Mac-1 (CD11b/CD18) up-regulation and systemic neutrophil activation during endotoxemia in vivo. *Journal of leukocyte biology* 1994; 55: 105-111.

161. Woodruff TM, Arumugam TV, Shiels IA, Reid RC, Fairlie DP, Taylor SM: Protective effects of a potent C5a receptor antagonist on experimental acute limb ischemia-reperfusion in rats. *Journal of Surgical Research* 2004; 116: 81-90.

162. Woolbright BL, Jaeschke H: The impact of sterile inflammation in acute liver injury. *Journal of clinical and translational research* 2017; 3: 170-188.

163. Woreta TA, Alqahtani SA: Evaluation of abnormal liver tests. *Medical Clinics* 2014; 98: 1-16.

164. Xia Y, Borland G, Huang J, Mizukami IF, Petty HR, Todd RF, et al.: Function of the lectin domain of Mac-1/complement receptor type 3 (CD11b/CD18) in regulating neutrophil adhesion. *The Journal of Immunology* 2002; 169: 6417-6426.

165. Xian W, Wu J, Li Q, Du X, Wang N, Chen D, et al.: CXCR3 alleviates renal ischemia-reperfusion injury via increase of Tregs. *Molecular Medicine Reports* 2021; 24: 1-9.

166. Zhai Y, Petrowsky H, Hong JC, Busuttil RW, Kupiec-Weglinski JW: Ischaemia–reperfusion injury in liver transplantation—from bench to bedside. *Nature reviews Gastroenterology & hepatology* 2013; 10: 79-89.

167. Zhang Q, Raoof M, Chen Y, Sumi Y, Sursal T, Junger W, et al.: Circulating mitochondrial DAMPs cause inflammatory responses to injury. *Nature* 2010; 464: 104-107.

168. Zheng Y, Cui B, Sun W, Wang S, Huang X, Gao H, et al.: Potential Crosstalk between Liver and Extra-liver Organs in Mouse Models of Acute Liver Injury. *International journal of biological sciences* 2020; 16: 1166-1179.

169. Zhou Z, Xu M-J, Gao B: Hepatocytes: a key cell type for innate immunity. *Cellular & molecular immunology* 2016; 13: 301-315.

170. Zilkens C, Friese J, Köller M, Muhr G, Schinkel C: HEPATIC FAILURE AFTER INJURY–ACommon PATHOGENESIS WITH SCLEROSING CHOLANGITIS? *Eur J Med Res* 2008; 13: 309-313.

171. Zonfrillo MR, Spicer RS, Lawrence BA, Miller TR: Incidence and costs of injuries to children and adults in the United States. *Injury epidemiology* 2018; 5:1-6.

7 Acknowledgements

The content has been removed for data privacy protection.

8 Curriculum Vitae

The content has been removed for data privacy protection.

Declaration

I hereby declare that I am the sole author of this doctoral thesis

The Inflammatory Response of the Liver after Polytrauma Promotes the Increase in the Secretion of Bone-related Modifiers

and that I have not used any sources other than those listed as references. This work has not yet been submitted to another examination institution – neither in Germany nor outside Germany – neither in the same nor in a similar way and has not yet been published and I have acknowledged all main sources of help.
I further hereby declare that I have conducted my academic work according to the principles of good scholarly and scientific practice and in accordance with the valid “Article of the University of Ulm for Ensuring Good Scientific Practice”.

Ulm 1 September 2022

Yang Li